XIII. STATISTICAL COMMUNICATION THEORY*

Prof. Y. W. Lee
Prof. A. G. Bose
Prof. I. M. Jacobs
Prof. D. J. Sakrison
Prof. M. Schetzen
Prof. H. L. Van Trees, Jr.
V. R. Algazi
A. A. Al-Shalchi
R. Alter
D. S. Arnstein
M. E. Austin
R. F. Bauer
J. D. Bruce
A. M. Bush
J. K. Clemens
D. F. DeLong, Jr.
A. F. Gann
E. P. Gould
C. E. Gray
H. Hemami
W. F. Kelly
P. L. Konop
V. S. Mummert
R. B. Parente
H. C. Salwen
T. L. Stewart
L. C. Thomas
C. E. Wernlein, Jr.
W. S. Widnall
R. W. Witte

A. WORK COMPLETED

1. METHODS OF DETERMINING COEFFICIENTS FOR OPTIMUM SYSTEMS

This study has been completed by H. C. Salwen. In May 1962, he submitted the results to the Department of Electrical Engineering, M.I.T., as a thesis in partial fulfillment of the requirements for degree of Master of Science.

M. Schetzen

2. SYNTHESIS OF SEVERAL SETS OF ORTHOGONAL FUNCTIONS

The present study has been completed by R. W. Witte. It was submitted as a thesis in partial fulfillment of the requirements for the degree of Master of Science, Department of Electrical Engineering, M.I.T., May 1962.

M. Schetzen

3. THRESHOLD STUDY OF PHASE-LOCKED LOOPS

The present study has been completed by M. Austin and the results have been presented to the Department of Electrical Engineering, M.I.T., as a thesis in partial fulfillment of the requirements for the degree of Master of Science.

H. L. Van Trees, Jr.

B. A TWO-STATE MODULATION SYSTEM

It is well known that two-state signals have advantages over continuous signals with respect to processing in electronic circuits. The former are much less sensitive to many variations in the parameters of the electronic devices because only the signal zero crossings are important. In particular, the linearity of the devices is of no concern.

*This work was supported in part by the National Institutes of Health (Grant MH-04737-02).

Also, high power level two-state signals can be handled with very high efficiency, since all of the active circuit elements can be operated in a switching mode with a consequent low power consumption.

Thus one can envision the usefulness of a simple method for converting a continuous signal into a two-state form in such a manner that the original signal can be recovered easily. Existing PCM and FM systems perform the conversion of continuous signals into two-state signals and vice versa; however, they are rather complex systems. The Delta modulation system achieves similar results with simpler equipment. This report describes a very simple modulation system that has, for particular applications, certain advantages over the above-mentioned systems.

The basic modulation system is depicted in Fig. XIII-1. The network N in the feedback loop can take on different forms that depend upon the desired modulator characteristics. In both the analytical and experimental studies, thus far, most of our attention has been devoted to the form of N consisting of a delay line followed by an integrator as shown in Fig. XIII-2. Analysis of the modulation system shows that with this type of feedback network the system oscillates in such a manner that

(a) With no signal input the output $y(t)$ is a square wave with a period T_0 controlled by the delay time T_d and the integrator time constant RC of the feedback network, and by the hysteresis width 2δ of the forward path.

(b) For any constant input the output is a rectangular wave with a period greater than T_0 and a duty cycle that is such that the average value of $y(t)$ is very nearly equal

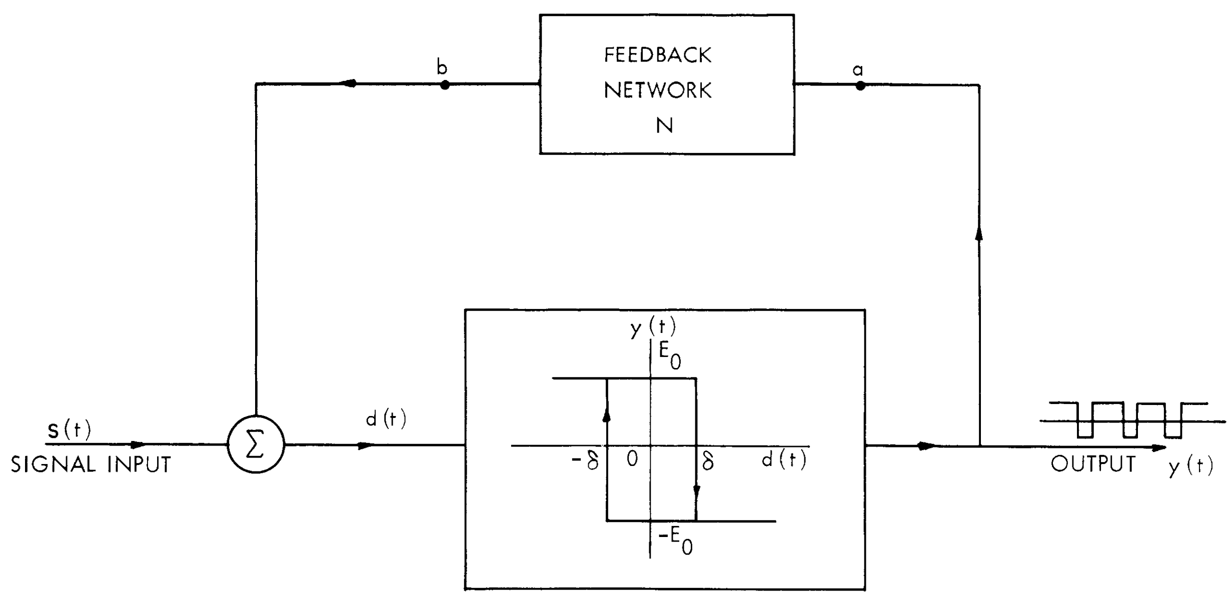

Fig. XIII-1. Diagram of the modulation system.

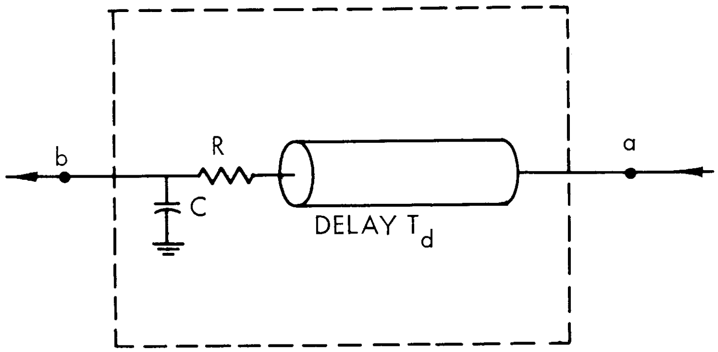

Fig. XIII-2. One form of the feedback network.

to the input signal.

(c) For slowly varying input signals S(t) the output exhibits a combination of frequency and pulse duration modulation in such a manner that S(t) can be recovered from the modulated signal by the simple operation of lowpass filtering.

The present system shares with Delta modulation the very simple method of demodulation. However, the present system does not exhibit a threshold effect or quantization noise in spite of the finite width of the hysteresis in the forward path. This result is to be expected because the Delta modulation output is quantized both in amplitude and time, whereas the output of the present system is quantized in amplitude only. On the other hand, the price that the present system pays for its freedom from quantization noise is that it is not useful in time-multiplexing systems.

The analysis of this system and some of its applications that are now under investigation will be presented in future reports.

A. G. Bose

C. DESIGN OF FILTERS FOR NON MEAN-SQUARE-ERROR PERFORMANCE CRITERIA BY MEANS OF A CONTINUOUS ADJUSTMENT PROCEDURE

1. Introduction

The problem considered in this report is that of designing a system containing k variable parameters, $x_1, x_2, \ldots, x_k$; the input to the system is a sample function v(t) from a stationary ergodic process and the desired output for the system is a sample function d(t) from a related stationary ergodic process. We shall not specify any relation between v(t) and d(t). This allows us to consider simultaneously the model problem [d(t) is the output of some given system whose input is v(t)]; the prediction problem ($d(t) = v(t+\alpha)$, $\alpha > 0$); and the filter problem (v(t) represents some corrupted form of $d(t+\alpha)$, α being either ≥ 0 or < 0 and the corruption not being limited to additive noise).

For convenience, the k-tuple of parameters $(x_1, x_2, \ldots, x_k)$ will be denoted by the k-dimensional vector $\underline{x}$ and the output of the filter (or model or predictor) will be denoted by $q_{\underline{x}}(t)$ to indicate its dependence on $\underline{x}$. What we wish to find is the parameter setting $\underline{x}$ for which $q_{\underline{x}}(t)$ most closely resembles d(t) is some prescribed sense. We measure this performance by attempting to minimize

$$M(\underline{x}) = E\{W[d_t - q_{\underline{x},t}]\}$$

in which W is a non-negative weighting function on the error, $e(t) = d(t) - q_{\underline{x}}(t)$. Normally W(e) is taken to be $(e)^2$ for ease of analytical treatment. Here we require only that W be strictly convex; subject to this restriction, it can be chosen to best express the purpose of the application. This problem will not admit of an easy analytic solution for a general convex function W, and thus we resort to an adjustment procedure; that is, we start the system with some initial parameter setting and observe how the performance of the system changes with certain perturbations of the k parameters $x_1, \ldots, x_k$. This information is then fed back to make changes in the parameter setting. We have already described[1] a method in which the parameters were perturbed sequentially and the adjustments in setting were made at discrete instants of time. In the method described here, simultaneous perturbations of the parameters are made and the parameter setting is continuously adjusted. The present continuous adjustment method described warrants consideration in that it can be realized with only simple analog computing facilities, while the discrete adjustment procedure requires digital computing equipment.

An adjustment method is of no use unless it can be guaranteed a priori that the parameter setting $\underline{x}$ will converge to the optimum setting. After describing the adjustment procedure, we shall state a set of assumptions concerning the processes involved and show that these guarantee convergence of $\underline{x}$ to the optimum setting in the mean-square sense.

Before describing the adjustment process, we introduce the necessary notation. The Euclidean inner product $\sum_{i=1}^{k} x_i y_i$ is denoted by $(\underline{x}, \underline{y})$, and the k-dimensional Euclidean norm by $\|\underline{x}\| = +[(\underline{x}, \underline{x})]^{1/2}$. A unit setting of the i^{th} parameter, x_i, and zero setting of the other k - 1 parameters will be denoted by $\underline{e}_i$, i = 1, 2, ..., k. For notational simplicity, we shall denote

$$Y_{\underline{x}}(t) = W[d(t) - q_{\underline{x}}(t)] \tag{1}$$

and also denote by $\underline{\theta}$ the optimum parameter setting; that is, the setting $\underline{x}$ that minimizes

$$M(\underline{x}) = E\{Y_{\underline{x},t}\}. \tag{2}$$

2. Description of the Adjustment Procedure and Conditions for Convergence

We shall consider only the design of filters (or predictors or models) of the form shown in Fig. XIII-3. This form is general in that if a sufficiently large number of $f_i(t)$ are chosen in a proper systematic manner, the filter can approximate arbitrarily closely any nonlinear operator whose output depends only negligibly on the remote past.[2] Furthermore, if a good filter is already available, it may be incorporated into the filter of Fig. XIII-3 by letting the signal $f_1(t)$ be the output of the given filter. For the parameter setting $x_1 = 1$, $x_2 = x_3 = \dots = x_k = 0$, the over-all filter reduces to this original filter, and hence its performance must be at least as good as that of the original filter.

The continuous adjustment procedure to be considered is shown in Fig. XIII-4. This operational block diagram provides the clearest and most concise description of the adjustment procedure. The adjustment mechanism requires only integrators, time-variant gains, and W error-weighting transducers. Note that the adjustment procedure continuously makes simultaneous measurements of difference approximations for all k components of the gradient. The measurement of the i^{th} such component is given by

$$Y_i(t) = Y^{2i-1}(t) - Y^{2i}(t) = W\left[d(t) - \sum_{i=1}^{k} x_i(t)\, f_i(t) - c(t)\, f_i(t)\right]$$

$$- W\left[d(t) - \sum_{i=1}^{k} x_i(t)\, f_i(t) + c(t)\, f_i(t)\right]. \tag{3}$$

The adjustment of the i^{th} parameter is then governed by

$$x_i(t) = x_i(1) - \int_1^t a(\tau)\, \frac{1}{c(\tau)} Y_i(\tau)\, d\tau. \tag{4}$$

Note that the measurement $\frac{1}{c(t)} Y_{i,t}$ is not the difference approximation itself but rather a random variable whose mean is a difference approximation to the i^{th} component of the gradient; that is, the difference approximation would be obtained by taking a long time average of $\frac{1}{c} Y_i(t)$ for fixed $\underline{x}$ and c.

This procedure is thus essentially a gradient-seeking procedure carried out in the presence of random fluctuations. In making the adjustment we are attemption to measure the direction of steepest descent and change the parameter setting in that direction. Because the adjustment process is essentially a gradient-seeking method, its usefulness is limited to systems and error-weighting functions for which $M(\underline{x})$ possesses a unique minimum. To be more precise, we require

$$\left(\operatorname{grad} M(\underline{z})\Big|_{\underline{z}=\underline{x}}, \underline{x}-\underline{\theta}\right) \geq K_o \|\underline{x}-\underline{\theta}\|^2, \qquad K_o > 0 \tag{5}$$

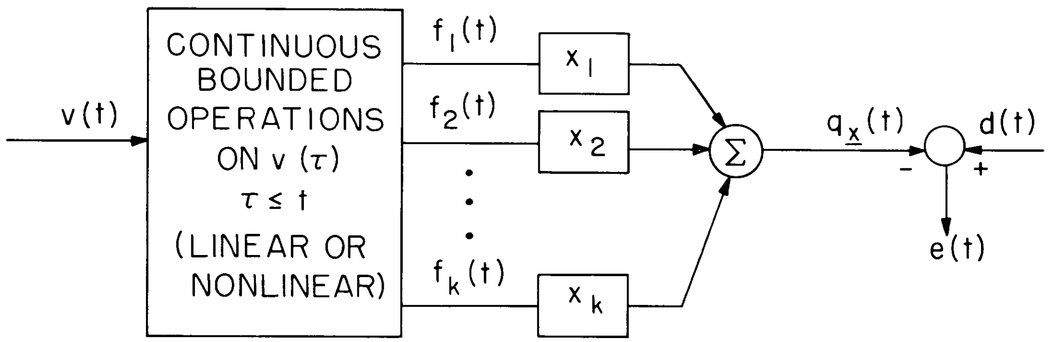

Fig. XIII-3. Form of the filter (or predictor or model) to be designed.

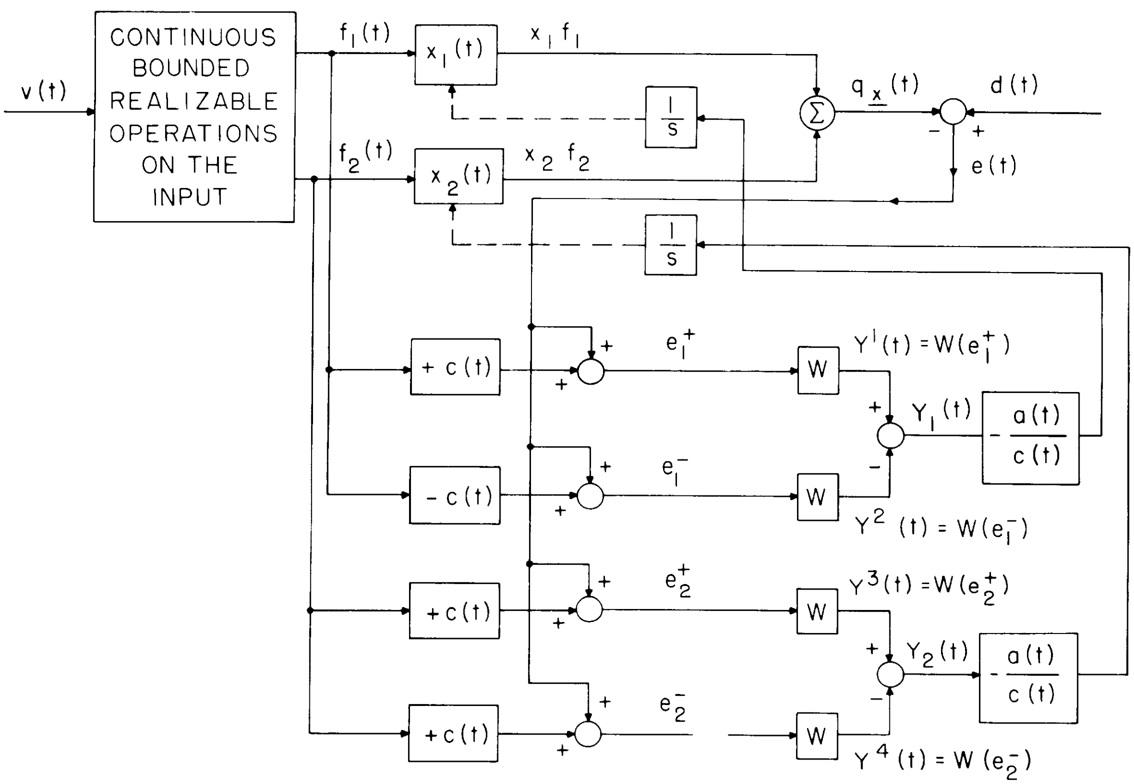

$$x_1(t) = x_1(1) - \int_1^t \frac{a(\tau)}{c(\tau)} Y_1(\tau)\, d\tau$$

$$x_2(t) = x_2(1) - \int_1^t \frac{a(\tau)}{c(\tau)} Y_2(\tau)\, d\tau$$

$$e_1^+ = -f_1(t)\left[x_1(t) + c(t)\right] - f_2(t)\, x_2(t) + d(t)$$

$$e_1^- = -f_1(t)\left[x\,(t) - c(t)\right] - f_2(t)\, x_2(t) + d(t)$$

$$e_2^+ = -f_1(t)\, x_1(t) - f_2(t)\left[x_2(t) + c_2(t)\right] + d(t)$$

$$e_2^- = -f_1(t)\, x_1(t) - f_2(t)\left[x_2(t) - c_2(t)\right] + d(t)$$

Fig. XIII-4. Diagram of the continuous adjustment procedure for two parameters, x_1 and x_2.

and

$$\left|\frac{\partial M(\underline{x})}{\partial x_i^3}\right| \leqslant Q, \qquad Q < \infty. \tag{6}$$

Inequality (5) simply means that, at any setting $\underline{x}$, the component of the gradient in the direction of the optimum setting is always less than $-K_0$ times the distance to the setting. Inequality (6) is self-explanatory. Inequality (5) prevents the adjustment from "sticking," while inequality (6) prevents sustained oscillations.

We wish to be able to state sufficient conditions directly on the procedure and processes involved which will guarantee convergence. The following are sufficient.

On the adjustment procedure we require:

(a) Let a(t) and c(t) be bounded, continuous, positive functions with the properties $\int_1^\infty a(t)\, dt = \infty$, $\int_1^\infty a(t)\, a\left(\frac{t}{2}\right) dt < \infty$, and $\int_1^\infty a(t)\, c^4(t)\, dt < \infty$.

(b) The parameter setting $\underline{x}$ is constrained to a bounded, closed, convex set X, but is free to be varied inside X. (A set X is convex if $\underline{x}_1 \in X$, $\underline{x}_2 \in X$ implies $\alpha\underline{x}_1 + (1-\alpha)x_2 \in X$ for $0 \leqslant \alpha \leqslant 1$.)

The following restrictions are sufficient to impose on the function W and the processes involved:

(c) The signals v(t) and d(t) are the outputs of stationary ergodic sources and are uniformly bounded in absolute magnitude for all t with probability one.

(d) The signals $f_i(t)$, $i = 1, 2, \ldots, k$, are obtained by bounded time-invariant operations on v(t) (and hence are also uniformly bounded in magnitude).

(e) The correlation coefficient between any $f_{i,t}$ and any linear combination of the remaining $f_{j,t}$ is different from plus or minus one; i.e., for any set of A_{ij}

$$\left| E\left\{ \frac{f_i - \bar{f}_i}{\sigma f_i} \cdot \frac{\sum\limits_{j=1\ \ j\neq i}^{k} A_{ij}(f_j - \bar{f}_j)}{\sigma \sum A_{ij} f_j} \right\} \right| < 1 \qquad i = 1, 2, \ldots, k$$

(f) The function W(e) is a polynomial of finite degree. Moreover, W(e) is to be "strictly convex" in the following sense: There exists an E greater than zero so that, for arbitrary a and b in the domain of W

$$W[\alpha a + (1-\alpha)b] \leqslant \alpha W[a] + (1-\alpha)\, W[b] - E\alpha(a-b)^2 \qquad 0 \leqslant \alpha \leqslant 1/2$$

(g) Consider the random processes d(t) and $f_i(t)$, $i = 1, 2, \ldots, k$. Let

$F_1[d(\tau_1), f_1(\tau_1), \ldots, f_k(\tau_1)]$ and $F_2[d(\tau_2), f_1(\tau_2), \ldots, f_k(\tau_2)]$ be any bounded continuous functionals of $d(t)$ and the $f_i(t)$ for $\tau_1 \leq t$ and $t + \alpha \leq \tau_2 \leq t + \alpha + T$, T fixed.

We then require for large α

$$\left|R_{F_1F_2}\right| = \left|E\{(F_1-\overline{F}_1)(F_2-\overline{F}_2)\}\right| \leq \frac{K}{\alpha^2}\sigma_{F_1}\sigma_{F_2}$$

in which $K < \infty$ and is independent of F_1 and F_2.

Before proceeding to the statements concerning the convergence of the adjustment procedure, let us comment on the nature of these restrictions. Restrictions (c)-(e) impose no serious limitation on our physical situation. Restriction (c) will surely be satisfied, since the output of any physical source is always uniformly bounded. Restriction (d) requires only that the filter be stable. Restriction (e) only requires that all the $f_i(t)$ differ from one another in the prescribed sense. The convexity requirement of (f) imposes the only serious limitation on the method. The polynomial restriction is no real limitation in addition to the convexity restriction, since any convex function is continuous and hence may be approximated arbitrarily closely over a finite range by a finite polynomial. Since the data are bounded, the error will always lie in a finite range. It should be noted that the inequality of restriction (f) is slightly stronger than the usual definition of strict convexity; in fact it requires that the polynomial W contain a nonzero quadratic term. By slightly strengthening restriction (e), we can weaken the inequality of (f) by requiring that it hold only for either a or b bounded away from zero. This will include any function W for which

$$0 < M_1 \leq W''(e) \leq M_2 \qquad \text{for } 0 < \epsilon \leq e \leq K < \infty$$

which includes $W(e) = |e|^p$, $p > 1$, and thus closely corresponds with the usual definition of strict convexity.[3]

To appreciate how inclusive the class of processes that satisfy restriction (g) is, refer to Fig. XIII-5. The quantity F_2 is obtained by an operation upon the data in the interval $t + \alpha \leq \tau \leq t + \alpha + T$. Now consider trying to predict F_2 by using some functional, F_1, on the data for $\tau \leq t$. Note that there is a complete separation of α seconds between the data used for F_1 and that used for F_2. Now the best linear prediction of F_2 given F_1 is

$$\widehat{F_2 - \overline{F}_2} = \frac{R_{F_1F_2}}{\sigma_{F_1}^2}(F_1-\overline{F}_1)$$

and the mean-square error in this prediction is

$$\frac{1}{\sigma_{F_1}^2}\left(\sigma_{F_1}^2\sigma_{F_2}^2 - R_{F_1F_2}^2\right).$$

Our requirement on $R_{F_1F_2}$ is thus a restriction on the rate of increase of the prediction error of the functional F_2 with increasing prediction time. In particular, for large prediction time we require that the prediction error approach its asymptotic value at a rate of $1/\alpha^4$. Note that if d_τ and the $f_{i,\tau}$, $t + \alpha_o \leq \tau \leq t + \alpha_o + T$ are statistically independent of d_τ and the $f_{i,\tau}$, $\tau \leq t$, then $R_{F_1F_2} = 0$ for $\alpha > \alpha_o$ and the inequality is satisfied. Restriction (e) will not, in general, be satisfied for a periodic process. Also, the rate

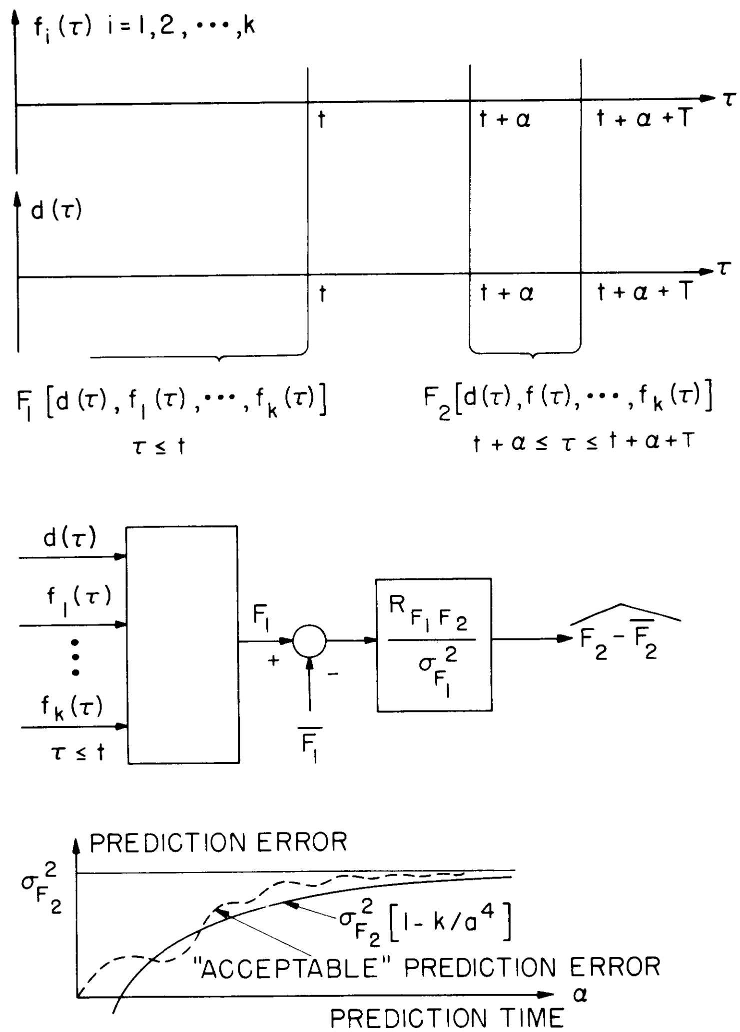

Fig. XIII-5. Explanation of restriction (e).

in restriction (e) could be reduced from $1/a^2$ to $1/a^{1+\epsilon}$, $\epsilon > 0$, although this would affect the rate of convergence given in Statement 2 below.

Having made the restrictions, we can now make the following statements concerning the convergence of the parameter setting, $\underline{x}_t$, to the optimum setting $\underline{\theta}$. The implication of these statements for the physical adjustment procedure is clear.

STATEMENT 1: Restrictions (a)-(g) imply the convergence of $\|\underline{x}_t-\underline{\theta}\|$ to zero in the mean-square sense for all allowable choices of initial parameter setting; that is,

$$\lim_{t\to\infty} E\left\{\|\underline{x}_t-\underline{\theta}\|^2\right\} = 0 \qquad \text{for all } \underline{x}(1) \in X.$$

We now set $a(t) = a/t^{\alpha}$ and $c(t) = c/t^{\gamma}$ for $t \geq 1$. In order to satisfy restriction (a) we require $1/2 < \alpha \leq 1$ and $\gamma > 1 - \alpha/4$. If $\alpha = 1$, we also require $a > 1/4K_o$, in which K_o is defined as in section 2. Under these conditions we can make the following statement.

STATEMENT 2: Restrictions (a)-(g) and the choice $\alpha = 1$, $\gamma > 1/4$ imply

$$E\left\{\|\underline{x}_t-\underline{\theta}\|^2\right\} \leq K\frac{1}{t}, \qquad K < \infty \qquad \text{for all } \underline{x}(1) \in X.$$

Moreover, no faster rate of convergence can be obtained which applies to all processes and error-weighting functions satisfying restrictions (a)-(g).

Relative to Statement 2, it should be pointed out that the given rate of convergence is the rate at which the parameter setting $\underline{x}_t$ approaches the optimum setting, $\underline{\theta}$, and not the rate at which the average performance, $M(\underline{x}_t)$, approaches the optimum, $M(\underline{\theta})$. However, since $M(\underline{x})$ is continuous, convergence of $\underline{x}_t$ to $\underline{\theta}$ insures the convergence of $M(\underline{x}_t)$ to $M(\underline{\theta})$. Note that it is not only the asymptotic rate of convergence which is important (1 in Statement 2), but also the initial convergence of $\underline{x}_t$ to a region near $\underline{\theta}$. This initial convergence depends critically on the adjustment coefficients a, c, α, and γ. Some studies[4,5] have been made in which the adjustment of these coefficients to obtain a rapid initial convergence is considered.

[Note: Proofs of Statements 1 and 2 will be given in Quarterly Progress Report No. 67, October 15, 1962.]

3. SIMPLE EXAMPLE

In order to give the reader a better feeling for restrictions (c)-(g), we present a simple example. We start with a familiar representation for a process and state conditions on the representation that will guarantee the satisfaction of restrictions (c)-(e) and (g).

The example is the unit prediction of a process v(t), which is generated in the following manner. Let white noise, $n(t)$, be passed through a linear device whose impulse response has the properties

$$|h_o(t)| \leq C_o' \qquad 0 \leq t \leq T_o$$

$$h_o(t) \equiv 0 \qquad t < 0,\ t > T_o.$$

Note that the output of this linear device could represent "shot noise" for a suitable choice of $h_o(t)$. The output of this linear device is passed through a limiter whose upper and lower limits are plus and minus L, respectively. Denote the output of the limiter by $w(t)$; the process $v(t)$ is then generated by passing $w(t)$ through another linear device with impulse response $h(t)$.

$$v(t) = \int_0^\infty h(\tau)\, w(t-\tau)\, d\tau \tag{7}$$

$$d(t) = v(t+1) \qquad \text{(unit prediction).} \tag{8}$$

The predictor will be a linear one of the form

$$\widehat{d(t)} = q_{\underline{x}}(t) = \sum_{i=1}^{k} x_i f_i(t) \tag{9}$$

in which

$$f_i(t) = \int_0^\infty h_i'(\tau)\, v(t-\tau)\, d\tau$$

or, if we let $h_i(t)$ denote the impulse response obtained by cascading (convolving) $h_i(t)$ and $h(t)$, then

$$f_i(t) = \int_0^\infty h_i(\tau)\, w(t-\tau)\, d\tau\,. \tag{10}$$

Now our assumptions on $h_o(t)$ and the limiter imply

(a) $|w_t| \leq L$ with probability one

w_t and $w_{t+\tau}$ are statistically independent for $\tau > T_o$.

We also make the assumptions:

$$\text{(b)}\quad |h(t)| \leqslant \begin{cases} 0 & t<0 \\ C_o < \infty & 0 \leqslant t \leqslant 1 \\ C_o/t^3 & t>1 \end{cases} \qquad |h_i(t)| \leqslant \begin{cases} 0 & t<0 \\ C_i < \infty & 0 \leqslant t \leqslant 1 \\ C_i/t^3 & t>1 \end{cases}$$

$$i = 1, 2, \ldots, k.$$

(c) The $h_i(t)$ are linearly independent in the sense that for any set of numbers A_{ij}

$$\left| \int_0^\infty h_i(\tau_1) \sum_{\substack{j=1\\ j\neq i}}^{k} A_{ij} h_j(\tau_2)\, R_{ww}(\tau_2-\tau_1)\, d\tau_1 d\tau_2 \right| < \int_0^\infty \int_0^\infty h_i(\tau_1)\, h_i(\tau_2)\, R_{ww}(\tau_2-\tau_1)\, d\tau_1 d\tau_2$$

$$\cdot \int_0^\infty \int_0^\infty [A_{ij} f_j(\tau_1)] \left[\sum_{\substack{j=1\\ j\neq i}}^{k} A_{ij} f_j(\tau_2) \right] R_{ww}(\tau_2-\tau_1)\, d\tau_1 d\tau_2$$

for $i = 1, 2, \ldots, k$, and $R_{ww}(\tau_1-\tau_2) = E\left\{ w_{t+\tau_1} w_{t+\tau_2} \right\}$.

We now wish to show that the assumptions (a)-(c) above guarantee the satisfaction of restrictions (c)-(e) and (g). Both (c) and (d) follow directly from assumption (a) and from the fact that assumption (b) implies

$$\int_0^\infty |h(t)|\, dt \leqslant 2C_o \qquad \int_0^\infty |h_i(t)|\, dt \leqslant 2C_i \qquad i = 1, 2, \ldots, k.$$

Assumption (c) is merely restriction (e) rephrased in terms of the predictor impulse responses.

We now turn to the problem of showing that restriction (g) is satisfied. In a future report (Quarterly Progress Report No. 67) it will be shown that in establishing Statements 1 and 2 we shall need to consider only functional quantities of the form

$$F_{1,t} = (x_t)^{r-1}\, Y_t \tag{11}$$

$$F_{2,t+a} = (f_{t+a})^p\, (d_{t+a})^s. \tag{12}$$

In the multidimensional case F_1 and F_2 are of the same form but contain all of the $f_i(t)$ and all of the components of $\underline{x}(t)$. We shall now demonstrate that restriction (g) is satisfied for the quantities given by Eqs. 11 and 12; the multidimensional case may be handled in the same manner, the added difficulty being only one of notation. Using Eqs. 7, 8, and 9, we may express F_2 as

$$F_2 - \overline{F}_2 = \int_0^\infty \int_0^\infty \dots \int_0^\infty h_1(\tau_1) \dots h_1(\tau_p)\, h(\tau_{p+1}) \dots h(\tau_{p+s})$$

$$\cdot \left[\zeta_{\tau_1 \dots \tau_{p+s}} - \overline{\zeta}_{\tau_1 \dots \tau_{p+s}}\right] d\tau_1 \dots d\tau_{p+s} \tag{13}$$

in which

$$\zeta_{\tau_1 \dots \tau_{p+s}} = w(t+a-\tau_1) \dots w(t+a-\tau_p)\, w(t+a+1-\tau_{p+1}) \dots \cdot w(t+a+1-\tau_{p+s}). \tag{14}$$

Thus

$$\overline{(F_{1,t}-\overline{F}_1)(F_{2,t+a}-\overline{F}_2)} = \overline{F_{1,t}(F_{2,t+a}-\overline{F}_2)}$$

$$= \int_0^\infty \dots \int_0^\infty h_1(\tau_1) \dots h_1(\tau_p)\, h(\tau_{p+1}) \dots h(\tau_{p+s})$$

$$\overline{F_{1,t}\left[\zeta_{\tau_1 \dots \tau_{p+s}} - \overline{\zeta}_{\tau_1 \dots \tau_{p+s}}\right]}\, d\tau_1 \dots d\tau_{p+s}. \tag{15}$$

The multiple integral of this equation can be broken up into p + s similar integrals, the first of which is

$$I_1 = \int_0^\infty \int_{\tau_1}^\infty \dots \int_{\tau_1}^\infty h_1(\tau_1) \dots h_1(\tau_p)\, h(\tau_{p+1})$$

$$\dots h(\tau_{p+s})\, \overline{F_{1,t}\left[\zeta_{\tau_1 \dots \tau_{p+s}} - \overline{\zeta}_{\tau_1 \dots \tau_{p+s}}\right]}\, d\tau_1 \dots d\tau_{p+s}. \tag{16}$$

Now $F_{1,t}$ depends on w( ) only for $\tau \leq t$. From assumption (a) and Eq. 14 we see that $F_{1,t}$ and $\zeta_{\tau_1 \dots \tau_{p+s}}$ in Eq. 16 are therefore statistically independent for $\tau_1 \leq a - T_o$, and thus

$$\overline{F_{1,t}(\zeta-\overline{\zeta})} = 0 \qquad \tau_1 \leq a - T_o.$$

Furthermore, $|F_{1,t}(\zeta-\overline{\zeta})|$, by assumption, is bounded with probability one, say, by K_8, $K_8 < \infty$. Therefore

$$|I_1| \leq K_8 \int_{a-T_o}^\infty \int_0^\infty \dots \int_0^\infty |h_1(\tau_1)| \dots |h_1(\tau_p)|\, |h(\tau_{p+1})| \dots |h(\tau_{p+s})|\, d\tau_1 \dots d\tau_{p+s}$$

$$\leq K_8 \int_{a-T_o}^\infty |h_1(\tau_1)|\, d_1\left[\int_0^\infty |h_1(\tau)|\, d\tau\right]^{p-1} \left[\int_0^\infty |h(\tau)|\, d\tau\right]^s \tag{17}$$

and, from assumption (b),

$$|I_1| \leq K_9 \frac{1}{(\alpha - T_o)^2} \quad \text{or} \quad |I_1| \leq \frac{4K_9}{\alpha^2} \quad \text{for } \alpha > 2T_o.$$

The other terms in Eq. 15 can be treated in exactly the same manner, and yield the desired inequality for F_2 and F_1.

4. Conclusions

The adjustment method described in this report for filter, predictor, or model design has one distinct advantage over correlation methods; it is applicable to the rather broad class of convex error-weighting functions. It should be pointed out that this advantage disappears when it is known a priori that the processes v(t) and d(t) are jointly Gaussian; in this situation the filter that minimizes the mean-square error also minimizes the mean of any convex weighting function of the error.[6] A second advantage of the method is that it requires only a knowledge that the processes satisfy certain liberal restrictions and does not require detailed information of the process statistics.

It is true that the adjustment method described here does require the availability of the signals v(t) and d(t) for a reasonably long interval of time. However, successful application of correlation methods requires detailed information of the process statistics, or alternatively, long intervals of data from which to measure the necessary statistics. If the adjustment procedure is used to design a filter for use at the receiving end of a communication channel, a sample function, d(t), which is known at the receiver, must be sent over the channel in order to carry out the adjustment procedure.

The author wishes to express his deep appreciation to V. R. Algazi, Gian Carlo Rota, and H. L. Van Trees, Jr. for helpful commentary and suggestions.

D. J. Sakrison

References

1. D. Sakrison, Application of Stochastic Approximation Methods to System Optimization, Technical Report 391, Research Laboratory of Electronics, M.I.T., July 10, 1962.

2. N. Wiener, Nonlinear Problems in Random Theory (The Technology Press of Massachusetts Institute of Technology, Cambridge, Mass., and John Wiley and Sons, Inc., New York, 1958).

3. For a discussion of this point see D. Sakrison, Technical Report 391, *op. cit.*, Appendix A.5, p. 70.

4. H. Kushner, An Efficient Iterative Procedure for Locating the Optimum Operating Point of a Noisy System, Report 22G-0011, Lincoln Laboratory, M.I.T., December 7, 1959.

5. H. Kushner, Efficient Iterative Methods for Optimizing the Performance of Multi-Parameter Noisy Systems, Report 22G-0043, Lincoln Laboratory, M.I.T., October 20, 1960.

6. S. Sherman, Non-Mean-Square Error Criteria, Trans. IRE, Vol. IT-4, No. 3, pp. 125-128, September 1958.

D. NONLINEAR NO-MEMORY FILTERS OF A PRESCRIBED FORM

In this report we present some results concerning the relation between the characteristics of the message and of the noise when the filter has a specified form. We are interested in the problem of mean-square filtering for the class of no-memory filters, as shown in Fig. XIII-6.

We consider the case

$$x(t) = m(t) + n(t)$$

$$z(t) = m(t)$$

in which m(t), the message, and n(t), the noise, are statistically independent. It is known that the output of the optimum mean-square filter is the conditional mean of the message, given the input

$$y(t) = E[m_t/m_t+n_t], \tag{1}$$

in which m_t and n_t are the amplitude random variables at time t of the message and the noise, respectively.

If the input and the desired output are stationary, then the filter is time-invariant and the output y(t) can be labelled g(x).

Equation 1 becomes

$$g(x) = \int_{-\infty}^{+\infty} u\, p_{m/m+n}(u/x)\, du. \tag{2}$$

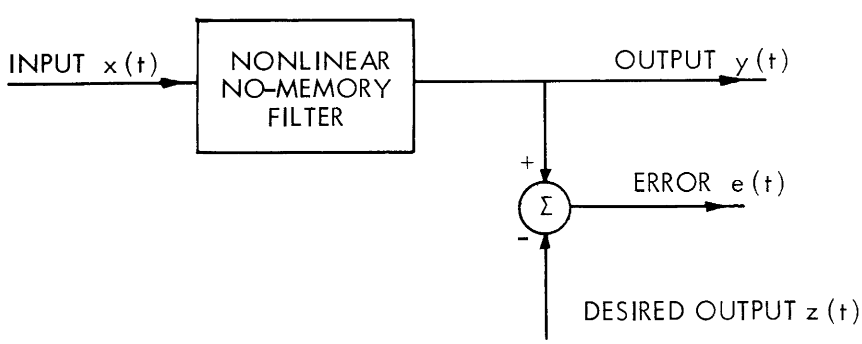

Fig. XIII-6. Filter operation considered.

By the use of Bayes' rule and by taking into account the fact that the message and the noise are statistically independent, g(x) can be written in the form

$$g(x) = \frac{\int_{-\infty}^{+\infty} u p_n(x-u)\, p_m(u)\, du}{\int_{-\infty}^{+\infty} p_n(x-v)\, p_m(v)\, dv}. \tag{3}$$

Let

$$r(x) \triangleq \int_{-\infty}^{+\infty} u\, p_n(x-u)\, p_m(u)\, du$$

$$q(x) \triangleq \int_{-\infty}^{+\infty} p_n(x-v)\, p_m(v)\, dv\ .$$

Hence, Eq. 3 can be written

$$g(x) = \frac{r(x)}{q(x)}. \tag{4}$$

Note that $q(x) = p_{m+n}(x)$.

We shall now express r(x) and g(x) in terms of the characteristic functions $P_n(t)$ and $P_m(t)$. We use the definitions:

$$p(u) = \frac{1}{2\pi} \int_{-\infty}^{+\infty} P(t)\, e^{-jtu}\, dt$$

$$P(t) = \int_{-\infty}^{+\infty} p(u)\, e^{jtu}\, du\ .$$

Writing r(x) in terms of $P_m(t)$ and $P_n(t)$, we obtain

$$r(x) = \int_{-\infty}^{+\infty} \int_{-\infty}^{+\infty} u\, p_m(u) \frac{P_n(t)}{2\pi}\, e^{-jt(x-u)}\, dt\, du$$

$$= \frac{1}{2\pi} \int_{-\infty}^{+\infty} P_n(t)\, e^{-jtx}\, dt \int_{-\infty}^{+\infty} u\, p_m(u)\, e^{jtu}\, du$$

$$r(x) = \frac{1}{2\pi} \int_{-\infty}^{+\infty} P_n(t) \frac{dP_m(t)}{d(jt)}\, e^{-jtx}\, dt$$

and

$$q(x) = \frac{1}{2\pi} \int_{-\infty}^{+\infty} P_n(t)\, P_m(t)\, e^{-jtx}\, dt\ . \tag{5}$$

Hence

$$g(x) = \frac{\int_{-\infty}^{+\infty} P_n(t) \frac{dP_m(t)}{d(jt)} e^{-jtx}\, dt}{\int_{-\infty}^{+\infty} P_n(t)\, P_m(t)\, e^{-jtx}\, dt}. \tag{6}$$

In the following discussion we shall use expressions (3) and (6) that we have just obtained for $g(x)$.

1. The Optimum Nonlinear No-Memory Filter Reduced to an Attenuator

If the optimum filter is $g(x) = ax$, the input signal is just attenuated, and Eq. 4 becomes $ax\, q(x) = r(x)$. By equating the Fourier transforms of both sides, we have, in terms of the characteristic functions,

$$\frac{a}{j} \frac{d}{dt} [P_n(t)\, P_m(t)] = P_n(t) \frac{dP_m(t)}{d(jt)}$$

and

$$\frac{dP_m(t)}{dt} P_n(t)[1-a] = aP_m(t) \frac{dP_n(t)}{dt}. \tag{7}$$

This linear differential equation (7) relating the characteristic functions of message and noise was obtained and discussed by Balakrishnan,[1] who used a different derivation.

The solution of (7) is

$$P_m(t) = [P_n(t)]^{a/1-a}. \tag{8}$$

If $P_n(t)$ is given, Eq. 8 establishes the corresponding $P_m(t)$ so that the attenuator with attenuation constant a is optimum.

If $P_m(t)$ is a characteristic function, it is necessary that $\frac{a}{1-a} \geqslant 0$, hence $0 \leqslant a \leqslant 1$. This condition can be shown by using the following properties of characteristic functions

$$\left.\begin{aligned} &P(0) = 1 \\ &|P(t)| \leqslant 1 \qquad \text{for } t \neq 0 \\ &P(-t) = P^*(t) \end{aligned}\right\} \tag{9}$$

in which $P^*(t)$ is the complex conjugate of $P(t)$.

We proceed with the discussion of Eq. 8 by looking for the classes of messages and noises which satisfy Eq. 8, and for which, independently of the noise level, the optimum filter is an attenuator. The solutions of Eq. 8 which satisfy this new condition are more significant from an engineering point of view.

If the noise level is changed,

$$p_n(u) \longrightarrow \frac{1}{c} p_n\left(\frac{u}{c}\right) \qquad c \geq 0$$
$$P_n(t_1) \longrightarrow P_n(ct_1) .$$

We assume that Eq. 8 is satisfied for a given noise and that, for $c = 1$,

$$P_m(t_1) = [P_n(t_1)]^{k_1} \qquad k_1 \triangleq \frac{a}{1-a} \geq 0 .$$

If the noise level is changed and the message stays unchanged, and if the optimum filter is still an attenuator, we have

$$P_m(t_1) = [P_n(ct_1)]^{k_2} \qquad k_2 \geq 0.$$

Hence

$$P_n(t_1) = [P_n(ct_1)]^k , \tag{10}$$

in which $k \triangleq \frac{k_1}{k_2} \geq 0$. Equation 10 expresses a relation between c and k which should hold for all t.

By differentiation, we obtain

$$kP_n'(ct_1) [P_n(ct_1)]^{k-1} t_1 \, dc + [P_n(ct_1)]^k \ln [P_n(ct_1)] \, dk = 0,$$

in which $P_n'(x)$ indicates differentiation with respect to the argument, x.

Letting $ct_1 = t$, we have

$$-\frac{k\,dc}{c\,dk} = \frac{P_n(t) \ln P_n(t)}{P_n'(t)\, t} \triangleq A,$$

in which A is independent of t.

If k and c are both positive and real, A is real. We have, therefore, an equation for $P_n(t)$:

$$\frac{P_n(t) \ln P_n(t)}{P_n'(t)\, t} = A . \tag{11}$$

Let

$$P_n(t) = \rho(t)\, e^{j\theta(t)}$$
$$\ln P_n(t) = \ln \rho(t) + j\theta(t)$$

Equation 11 becomes

$$\frac{\ln \rho(t) + j\theta(t)}{\frac{\rho'(t)}{\rho(t)} + j\theta'(t)} = At$$

or

$$\ln \rho(t) + j\theta(t) = At\frac{\rho'(t)}{\rho(t)} + jAt\theta'(t).$$

Thus

$$\left.\begin{aligned} \ln \rho(t) &= At\frac{\rho'(t)}{\rho(t)} \\ \theta(t) &= At\theta'(t), \end{aligned}\right\} \tag{12}$$

which can be solved to give

$$|\theta(t)| = D|t|^{1/A}$$

$$\rho(t) = e^{-B|t|^{1/A}} \qquad B \geq 0.$$

Here, we have used conditions (9). By another use of conditions (9) the solutions that are possible characteristic functions reduce to

$$P_n(t) = e^{-B|t|^k} \qquad 0 \leq k \leq 2 \tag{13a}$$

$$P_n(t) = e^{-B|t|}\, e^{jDt} \tag{13b}$$

in which B is real and positive and D is real. The condition $0 \leq k \leq 2$ for this type of characteristic function has been given by Schetzen.[2]

The characteristic functions represented by (13a) correspond to density functions with zero mean, among which are the Gaussian and Cauchy density functions ($k = 2$ and $k = 1$, respectively).

The characteristic function represented by (13b) corresponds to the Cauchy density function with mean D.

$$p_n(u) = \frac{1}{\pi}\frac{B}{B^2 + (u-D)^2}.$$

We note that the following characteristic functions, which were considered by Balakrishnan, satisfy Eq. 8:

The discrete Poisson distribution with characteristic function

$$P(t) = e^{\lambda(e^{jt}-1)}$$

and the continuous Γ type of density with characteristic function

$$P(t) = [1-cjt]^{-\gamma} \qquad \gamma, c > 0.$$

However, consider the noise with characteristic function $P_n(t) = [1-cjt]^{-\gamma}$. The corresponding message, if the filter is an attenuator with attenuation constant a, has, for its characteristic function,

$$P_m(t) = [1-cjt]^{-\gamma a/(1-a)}.$$

If we change the noise level and let

$$P_n(t) \longrightarrow P_n(kt) = [1-kcjt]^{-\gamma},$$

the optimum filter is no longer an attenuator, although the noise is still of the Γ type. Note that if $P_n(t) = P_m(t)$, Eq. 8 is always satisfied with $a = \frac{1}{2}$, whatever $P_m(t)$.

2. The Optimum Nonlinear No-Memory Filter of Prescribed Form

This problem has been considered quite generally by Balakrishnan. For mean-square filtering and no-memory filters, his approach leads to a differential equation relating the characteristic functions of the message and the noise whenever the filter g(x) has the form of a specified polynomial in x. We shall extend this result to the case in which g(x) is a ratio of polynomials.

Recently, Tung[3] has obtained the probability density of the input of the optimum filter as a function of the filter characteristic g(x) when the noise is Gaussian. We shall establish necessary relations between the input density and the filter characteristic when the noise is Poisson or of the Γ type.

We use expression (4) and the Fourier transforms of r(x) and q(x) which are

$$R(t) = P_n(t) \frac{dP_m(t)}{d(jt)}$$

$$Q(t) = P_n(t)\, P_m(t)\ .$$

a. Filter characteristic g(x), a ratio of polynomials

$$g(x) = \frac{\sum_{k=0}^{M} a_k x^k}{\sum_{\ell=0}^{N} b_\ell x^\ell}\ .$$

Hence

$$\left[\sum_{k=0}^{M} a_k x^k\right] q(x) = \left[\sum_{\ell=0}^{N} b_\ell x^\ell\right] r(x)\ .$$

By equating the Fourier transforms,

$$\sum_{k=0}^{M} a_k \frac{d^k[P_n(t)\, P_m(t)]}{[d(jt)]^k} = \sum_{\ell=0}^{N} b_\ell \frac{d^\ell \left[P_n(t)\, \frac{dP_m(t)}{d(jt)}\right]}{[d(jt)]^\ell} .$$

If we know the characteristic function of the noise, this is a linear differential equation with variable coefficients for the characteristic function of the message.

b. Relation between the input density function and the filter characteristic for various types of noise

Consider again Eq. 4, which, by writing r(x) in terms of its Fourier transform, may be written

$$g(x)\, q(x) = \frac{1}{2\pi} \int_{-\infty}^{+\infty} P_n(t)\, \frac{dP_m(t)}{d(jt)}\, e^{-jtx}\, dt, \tag{14}$$

but we can write

$$P_n(t)\, \frac{dP_m(t)}{d(jt)} = \frac{d}{d(jt)} [P_n(t)\, P_m(t)] - P_m(t) \frac{dP_n(t)}{d(jt)} .$$

Since q(x) is the Fourier transform of $P_n(t)\, P_m(t)$, we have

$$[g(x)-x]\, q(x) = -\frac{1}{2\pi} \int_{-\infty}^{+\infty} P_m(t)\, \frac{dP_n(t)}{d(jt)} e^{-jtx}\, dt . \tag{15}$$

Comparison of (14) and (15) shows that if the characteristics of message and noise are interchanged, then the characteristic of the optimum filter is changed from g(x) to x - g(x). This is a general result holding for filters with memory, as well as non mean-square criteria (see Schetzen[4]).

We define F(t) as

$$\frac{dP_n(t)}{d(jt)} = F(t)\, P_n(t)$$

or

$$F(t) = \frac{d[\ln P_n(t)]}{d(jt)} .$$

Let f(x) be the Fourier transform of F(t). Then by transforming the right-hand side of Eq. 15, we obtain

$$[g(x)-x]\, q(x) = -\int_{-\infty}^{+\infty} q(x_1)\, f(x-x_1)\, dx_1 . \tag{16}$$

We shall now apply Eq. 16 to various types of noise. Since (16) is a homogeneous equation, $q(x) \equiv 0$ is a solution. This solution is of no interest here, and henceforth we shall assume that $q(x) \neq 0$.

For Gaussian noise,

$$P_n(t) = e^{-\frac{\sigma^2}{2} t^2}$$

and

$$\frac{d[\ln P_n(t)]}{d(jt)} = F(t) = -\frac{\sigma^2 t}{j} .$$

Hence

$$f(x) = -\sigma^2 u_1(x) ,$$

in which $u_1(x)$ is the unit doublet occurring at $x = 0$. Equation 16 now takes the form

$$[g(x)-x]\, q(x) = \sigma^2 \frac{dq(x)}{dx},$$

which can be integrated to give

$$q(x) = \exp\left[-\frac{1}{\sigma^2}\int [x-g(x)]\, dx\right] .$$

This is the expression obtained by Tung.[3]

For Poisson noise,

$$P_n(t) = e^{\lambda(e^{jt}-1)}$$

and

$$\frac{d[\ln P_n(t)]}{d(jt)} = F(t) = \lambda\, e^{jt} .$$

Therefore

$$f(x) = \lambda\, u(x-1) .$$

We denote by $u(x-1)$ the unit impulse occurring at $x = 1$. Equation 16 now takes the form

$$[g(x)-x]\, q(x) = -\lambda\, q(x-1) ,$$

which can be written

$$q(x+1) - A(x)\, q(x) = 0. \tag{17}$$

Here, we let

$$A(x) = \frac{\lambda}{x + 1 - g(x+1)} .$$

The solution of the difference equation (17) is well known.[5]

Let t(x) be an arbitrary single-valued function defined in a unit interval $a \leqslant x < a+1$. Then we have

$$q(x) = t(a_x)A(a_x)A(a_x+1) \ldots A(x-1) \qquad x \geqslant a,$$

in which a_x is the point in the interval $a \leqslant x < a+1$ which is such that $x - a_x$ is an integer.

For noise of the Γ type,

$$P_n(t) = [1-cjt]^{-\gamma} \qquad \gamma, \; c > 0$$

Hence

$$\frac{d[\ln P_n(t)]}{d(jt)} = F(t) = c\gamma[1-cjt]^{-1}$$

and

$$f(x) = \begin{cases} \gamma \, e^{-x/c} & x \geqslant 0 \\ 0 & x < 0 . \end{cases}$$

Now Eq. 16 takes the form

$$[g(x)-x] \, q(x) = - \int_{-\infty}^{x} q(x_1) \, \gamma \, e^{-(x-x_1)/c} \, dx_1 ,$$

which can be written

$$[x-g(x)] \, q(x) \frac{e^{x/c}}{\gamma} = \int_{-\infty}^{x} q(x_1) \, e^{x_1/c} \, dx_1 .$$

By differentiation,

$$\frac{d}{dx} \left\{ [x-g(x)] \, q(x) \, \frac{e^{x/c}}{\gamma} \right\} = q(x) \, e^{x/c} .$$

This is a differential equation for g(x) that can be written

$$\frac{dq(x)}{dx} \left\{ \frac{x-g(x)}{\gamma} \right\} + q(x) \left\{ \frac{1-g'(x)}{\gamma} + \frac{x-g(x)}{\gamma c} - 1 \right\} = 0 ,$$

in which

$$g'(x) = \frac{dg(x)}{dx} .$$

For $q(x) \neq 0$, we have

$$\frac{\frac{dq(x)}{dx}}{q(x)} = -\frac{1-g'(x)}{x-g'(x)} - \frac{1}{c} + \frac{\gamma}{x-g(x)},$$

and the expression for q(x) is

$$q(x) = \frac{B\, e^{-\frac{x}{c}}}{|x-g(x)|} \exp\left[\int \frac{\gamma\, dx}{x-g(x)}\right],$$

in which B is a positive constant.

If g(x), the characteristic of the nonlinear filter, is given and if the noise is of a type considered above, then q(x), the probability density of the input, has to fulfill the following conditions:

(i) q(x) has to satisfy the relation obtained in terms of g(x).

(ii) q(x) has to be a proper density function.

(iii) $P(t) = \frac{Q(t)}{P_n(t)}$ has to be a characteristic function, in which we let Q(t) be the characteristic function for q(x), and $P_n(t)$ be the characteristic function for the noise. The third requirement comes from the fact that

$$Q(t) = P_m(t)\, P_n(t),$$

in which $P_m(t)$ is the characteristic function of the message.

A simple verification of the relations obtained between the input density function and the filter characteristic can be made by taking g(x) = ax. We then know from the results of section 1 the relation between the message and the noise, and hence the characteristic of the input if the noise is known. Therefore, whenever the noise is Gaussian, Poisson or of the Γ type, and g(x) = ax, we have an alternate derivation of q(x), the probability density of the input.

V. R. Algazi

References

1. A. V. Balakrishnan, On the characterization of processes for which the optimal mean square systems are of specified form, Trans. IRE, Vol. PGIT-6, pp. 490-501, September 1960.

2. M. Schetzen, Fourier transforms of positive functions, Quarterly Progress Report No. 52, Research Laboratory of Electronics, M.I.T., January 15, 1959, p. 79.

3. F. Tung, Optimal message for zero memory systems with additive Gaussian noise, Proc. IRE 50, 481 (1962).

4. M. Schetzen, A property of optimum systems, Quarterly Progress Report No. 65, Research Laboratory of Electronics, M.I.T., April 15, 1962, p. 129.

5. See, for, instance, G. Boole, A Treatise on the Calculus of Finite Differences (Dover Publications, Inc., New York, 1960), p. 161.

E. METHODS OF DETERMINING COEFFICIENTS FOR OPTIMUM SYSTEMS

1. Introduction

Optimum linear systems can be determined analytically by solving the Wiener-Hopf equation. No simple analytical solutions exist for the nonlinear case because the integral equation to be solved involves higher-order correlation functions. In view of the complexity of the analytical approach to the nonlinear optimization problem, experimental optimization procedures seem to be advantageous. Two experimental optimization techniques are discussed in this report.

The response of an optimum system can be represented as the sum of the responses of several subsystems.[1] Each subsystem consists of a network and a gain coefficient. If the subsystems are linear, then the impulse response of any optimum linear system can be represented in the form

$$h_{opt}(t) = \sum_n a_n \theta_n(t) , \tag{1}$$

in which the a_n are the gain coefficients, and the $\theta_n(t)$ are the impulse responses of the subsystem. Similarly, if the subsystems are a set of nonlinear operators such as the G-functional set,[2] any optimum nonlinear operation can be represented as a weighted sum of the subsystem operations. In this way, any optimum system, linear or nonlinear, can be synthesized by a suitable choice of the gain coefficients a_n.

There are several methods for determining the optimum gain coefficients.[3,4] The most popular of these is the Method of Steepest Descent. This method is an iterative surface-searching procedure by which a given performance criterion can be maximized through sequential adjustment of the gain coefficients. It has been shown[3] that under ideal conditions the solutions obtained by this method converge to the optimum solutions

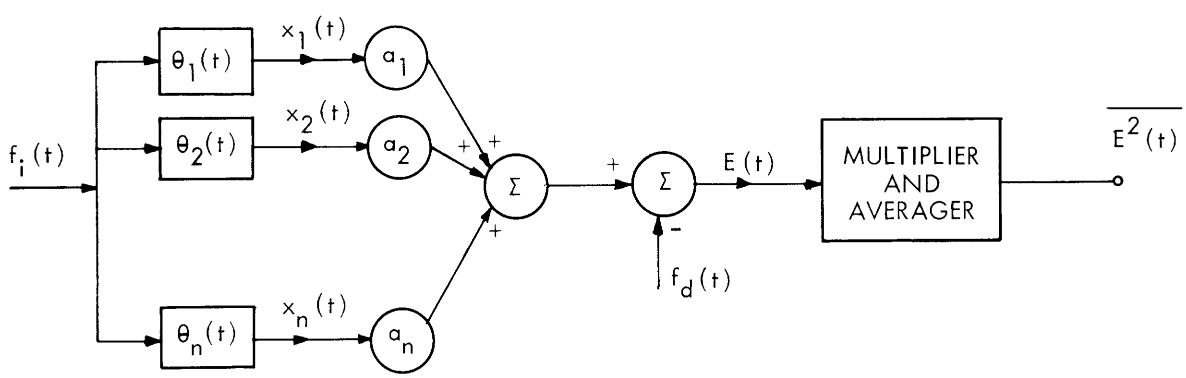

Fig. XIII-7. Basic optimization network.

at a rate $O(1/n^{1/2})$, where n is the number of iterations performed.

The Method of Steepest Descent is a general method. For instance, the procedure is the same regardless of the performance criterion chosen or the particular characteristics of the subsystems. We felt that the optimization could be performed more quickly and accurately if the experimental technique employed was designed specifically for a particular error criterion and a particular form of network. Throughout the analytical and experimental investigation of these techniques the performance criterion was always chosen to be the minimum mean-square error. The form of the network was always an operator expansion, as shown in Fig. XIII-7.

2. Optimization by Solving Simultaneous Equations

The mean-square error at the output of the network shown in Fig. XIII-7 is given by

$$\overline{E^2(t)} = \overline{[f_o(t)-f_d(t)]^2} = \overline{\left[\sum_n a_n x_m(t) - f_d(t)\right]^2} \quad . \tag{2}$$

A set of simultaneous equations which can be solved for the optimum gain coefficients is generated as follows: The mean-square error is differentiated with respect to each of the gain coefficients. Each of the derivatives is then set to zero to form N simultaneous equations for the gain coefficients.

$$\begin{aligned}
a_1\overline{x_1^2} + a_2\overline{x_1x_2} + \dots + a_N\overline{x_1x_N} &= \overline{x_1f_d} \\
a_1\overline{x_1x_2} + a_2\overline{x_2^2} + \dots + a_N\overline{x_2x_N} &= \overline{x_2f_d} \\
&\vdots \\
a_1\overline{x_1x_N} + \dots + a_N\overline{x_N^2} &= \overline{x_Nf_d} \, .
\end{aligned} \tag{3}$$

The correlation coefficients, $\overline{x_ix_j}$, $(i=1, 2, \dots, N)$, $(j=1, 2, \dots, N)$, and $\overline{x_if_d}$, $(i=1, 2, \dots, N)$ can be determined experimentally by multiplying the appropriate functions and averaging. Of course, the correlation coefficients are determined with some error, since the indicated averages cannot be performed over an infinite interval. In terms of the correlation coefficients, the optimum gain coefficients are given by

$$a_i = \frac{\begin{vmatrix} \overline{x_1^2} & \cdots & \overline{x_1 f_d} & \cdots & \overline{x_1 x_N} \\ \vdots & & & & \\ \overline{x_1 x_N} & \cdots & \overline{x_N f_d} & \cdots & \overline{x_N^2} \end{vmatrix}}{\begin{vmatrix} \overline{x_1^2} & \cdots & \overline{x_1 x_N} \\ \vdots & & \\ \overline{x_1 x_N} & \cdots & \overline{x_N^2} \end{vmatrix}} \qquad i = 1, 2, \ldots, N \tag{4}$$

Although this method is simple and direct, under certain conditions it will yield results that are unstable. That is, the normalized variances of the gain coefficients are much greater than the normalized variances of the correlation coefficients. This difference occurs when the crosscorrelation coefficients $\overline{x_i x_j}$, $i \neq j$, are large; that is, $\overline{x_i^2}\,\overline{x_j^2} \approx \overline{x_i x_j}^2$. Then the denominator determinant of (4) is the difference of the two large, but almost equal, numbers. The numbers are the sums of products of experimentally determined correlation coefficients. Since correlation coefficients are determined with some error, the numbers will be in error. Consequently, the error in the difference of the numbers will be large. Therefore, when two or more of the signals, $x_1(t)$, $x_2(t)$, ..., $x_N(t)$, are strongly correlated, the denominator determinant approaches zero, and the error in determining the optimum gain coefficients is large. The special case for which the network of Fig. XIII-7 consists of only two filters was analyzed in detail. It was found that the ratio of the normalized variance in the solution for a gain coefficient to the normalized variance in measurement of the correlation coefficients was inversely proportional to the fourth power of the denominator determinant of (4). Stable solutions can be obtained if all of the crosscorrelation coefficients are small. Therefore, it is desired that the outputs of the filters, $x_1(t)$, $x_2(t)$, ..., $x_N(t)$, be orthogonal.

3. Optimization by Orthogonalization

The set of signals $x_1(t), \ldots, x_N(t)$ can be orthogonalized by forming a new set of signals, $y_1(t), \ldots, y_N(t)$, in the following way:

$$\begin{aligned} y_1(t) &= x_1(t) \\ y_2(t) &= x_2(t) - a_{21} y_1(t) \\ y_3(t) &= x_3(t) - a_{31} y_1(t) - a_{32} y_2(t) \\ &\;\vdots \\ y_N(t) &= x_N(t) - a_{N1} y_1(t) - a_{N2} y_2(t) \ldots a_{NN-1} y_{N-1}(t) \,. \end{aligned} \tag{5}$$

The orthogonalization coefficients, a_{ij}, are determined sequentially to make $\overline{y_i(t)\, y_j(t)} = 0$ for $i \neq j$. The first coefficient, a_{21}, is determined by using the second equation of (5) and the condition that $\overline{y_1 y_2} = 0$. That is,

$$\overline{y_1 y_2} = 0 = \overline{x_2 y_1} - a_{21}\overline{y_1^2} \qquad \text{and} \qquad a_{21} = \frac{\overline{x_2 y_1}}{\overline{y_1^2}}. \tag{6}$$

Having determined a_{21} and $y_2(t)$, we can find a_{31} and a_{32} from the conditions $\overline{y_1 y_3} = \overline{y_2 y_3} = 0$.

$$\begin{aligned} \overline{y_1 y_3} &= 0 = \overline{x_3 y_1} - a_{31}\overline{y_1^2} - a_{32}\overline{y_1 y_2} \\ \overline{y_2 y_3} &= 0 = \overline{x_3 y_2} - a_{31}\overline{y_1 y_2} - a_{32}\overline{y_2^2}. \end{aligned} \tag{7}$$

The simultaneous equations, Eqs. 7, can be solved to determine a_{31} and a_{32} and thus $y_3(t)$. To determine $y_4(t)$, three simultaneous equations must be solved, and so on. Note that in solving Eqs. 7 it is not assumed that $\overline{y_1 y_2} = 0$. Since a_{21} is determined experimentally, $\overline{y_1 y_2}$ will be generally small but not zero. Note also that the solutions obtained from these simultaneous equations are stable because $\overline{y_i y_j}$, $i \neq j$, is always small.

When the set of signals $y_i(t)$ is completely constructed, a set of optimum gain coefficients can be determined by using Eqs. 4 (by changing all x_i to y_i).

Two methods have been presented: the method of optimization by solving simultaneous equations, and the method of optimization by orthogonalization. A statistical analysis of these methods was found to be very complicated. However, the expected value of the mean-square error was calculated for a special case – the system of Fig. XIII-7 consisting of only two subsystems. For this case, it was possible to determine that the rate of convergence of the expected value of the mean-square error was at least proportional to $1/T$ for either method. In general, the rate of convergence can be expected to be faster than that for the Method of Steepest Descent. Some insight into the characterisitcs of these procedures for the general N-filter case was gained from the analysis of the two-filter case. In particular, we found that for some problems, the solution obtained by the method of optimization by solving simultaneous equations was unstable. The method of optimization by orthogonalization is always stable, but it must be a sequential process. In fact, for a network with N subsystems, the orthogonalization method requires N cycles of (N+1) measurements. The method of optimization by solving simultaneous equations requires $\frac{1}{2}N(N+3)$ measurements. These can be performed simultaneously. This means that for a fixed averaging time and an unlimited number of correlation-coefficient calculators, the orthogonalization method takes approximately N times longer than the method of optimization by solving simultaneous equations. If from one to N correlation-coefficient calculators are available, the orthogonalization method still takes approximately twice as long for large N.

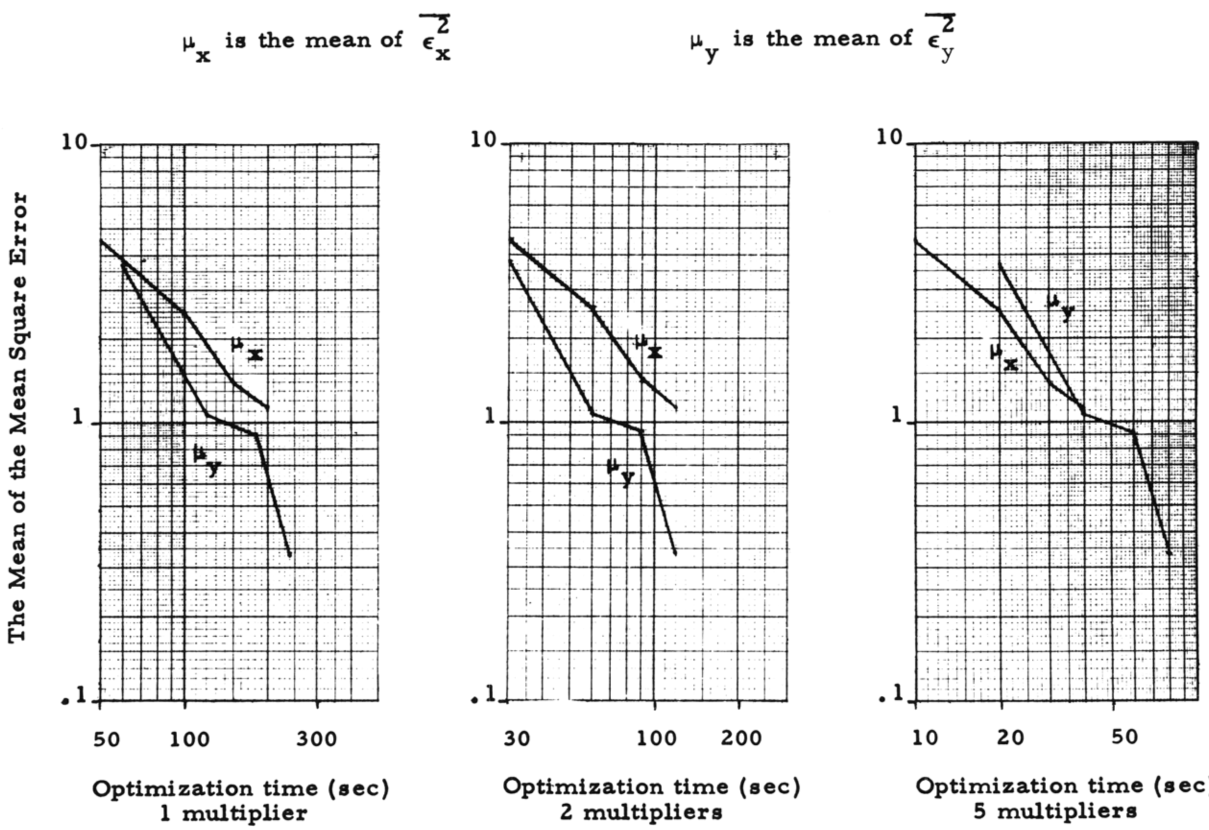

Fig. XIII-8. Mean of the mean-square error.

4. Experimental Comparison of Optimization Methods

An experiment demonstrating the operation and performance of the optimization methods for a special case — the network of Fig. XIII-7 consisting of only two linear subsystems — was carried out on a Philbrick Analog Computer in the Engineering Projects Laboratory, M.I.T. In this experiment, the frequency responses of the subsystems were

$$\theta_1(s) = \frac{10}{s+10}$$

and

$$\theta_2(s) = \frac{60 - 11.5s}{(s+10)^2}.$$

The input was Gaussian noise with power density spectrum given by

$$\Phi_{ii}(\omega) = \frac{\omega^2}{(\omega^2+1000)(\omega^2+400)}.$$

The desired output was constructed so that $f_d(t) = x_1(t) + x_2(t)$, where $x_1(t)$ and $x_2(t)$ are

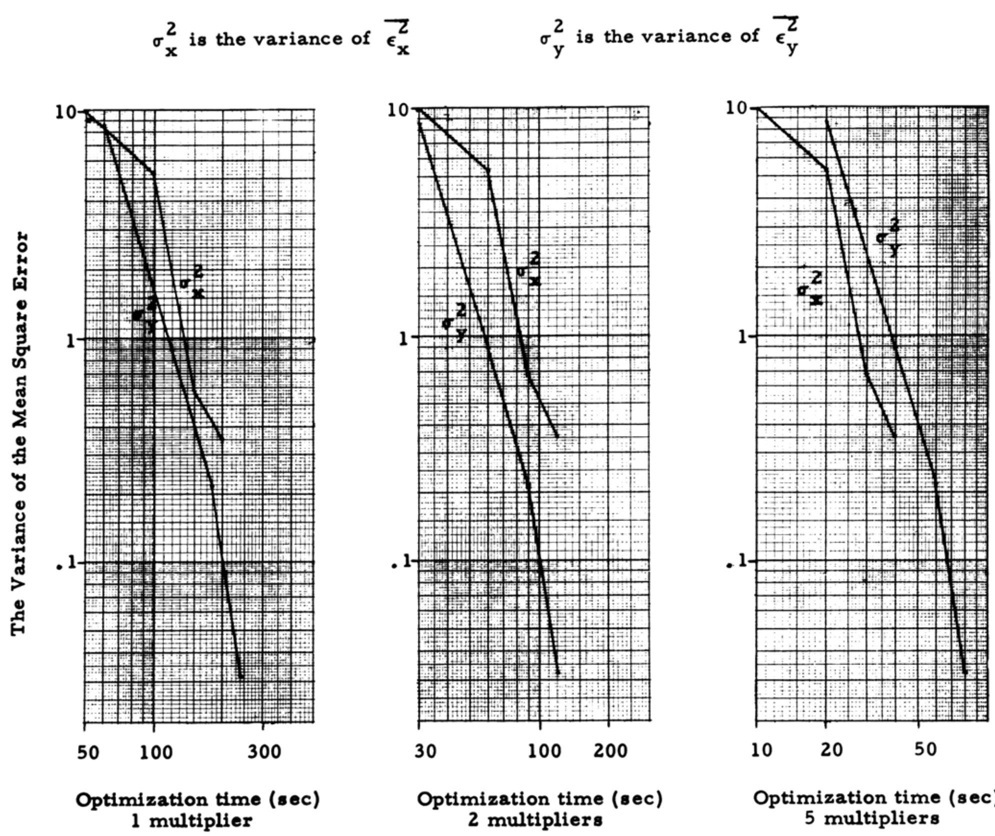

Fig. XIII-9. Variance of the mean-square error.

the outputs of the subsystems shown in Fig. XIII-7. The optimization experiment was performed many times under various conditions. Several values of the mean-square errors $\overline{\epsilon_x^2(t)}$, the mean-square error obtained by the method of optimization by solving simultaneous equations, and $\overline{\epsilon_y^2(t)}$, the mean-square error obtained by the orthogonalization method, were observed. The means and variances of these mean-square errors were compared as a function of the total optimization time and of the number of correlation-coefficient calculators (that is, multipliers) that were available. The total number of correlation-coefficient calculators required is a very practical criterion, since an accurate wideband multiplier is costly. The results are shown in Fig. XIII-8 and Fig. XIII-9.

The rate of convergence of the mean of the mean-square error for the method of optimization by solving simultaneous equations is roughly proportional to $1/T$ in all three cases considered in Fig. XIII-8, whereas the rate of convergence of the mean of the mean-square error for the method of optimization by orthogonalization is roughly proportional to $1/T^2$. The variance of the mean-square error for the method of optimization by solving simultaneous equations converges faster than $1/T^2$ for all three cases considered in Fig. XIII-9, whereas the variance of the mean-square error for the orthogonalization method converges faster than $1/T^3$.

5. Conclusions

The advantages of optimization by orthogonalization over optimization by solving simultaneous equations are not clear-cut. Consider two limiting conditions. If the outputs $x_1(t) \dots x_N(t)$ are almost orthogonal, the orthogonalization procedure is a waste of time. More accurate solutions can be obtained with the method of optimization by solving simultaneous equations directly. In this case, the direct solutions will be stable. On the other hand, if any one of the signals $x_1(t) \dots x_N(t)$ has a strong dependent component, then the solutions obtained by the direct method are unstable, and the orthogonalization method must be used.

The advantages of one method over the other are entirely a function of the network that is to be optimized and the specifications of the optimization problem. Therefore, if a system of the type described in this report is constructed, it should be adaptable to either of these optimization techniques. The two optimization techniques could then be applied in combination as follows: A quick examination of the outputs of the subsystems would determine which of the outputs must be orthogonalized to insure the stability of the solutions. Then the orthogonalization procedure would be used to orthogonalize only those signals with large dependent components.

H. C. Salwen

References

1. Y. W. Lee, Statistical Theory of Communication (John Wiley and Sons, Inc., New York, 1960).

2. N. Wiener, Nonlinear Problems in Random Theory (The Technology Press of Massachusetts Institute of Technology, Cambridge, Mass., and John Wiley and Sons, Inc., New York, 1958).

3. D. Sakrison, Application of Stochastic Approximation Methods to System Optimization, Technical Report 391, Research Laboratory of Electronics, M.I.T., July 10, 1962.

4. M. Schetzen, Some Problems in Nonlinear Theory, Technical Report 390, Research Laboratory of Electronics, M.I.T., July 6, 1962.

F. SYNTHESIS OF SEVERAL SETS OF ORTHOGONAL FUNCTIONS

1. Introduction

A set of networks was designed and constructed whose impulse responses comprise the first 12 terms of two orthogonal sets of functions, the Laguerre set and an exponential set, and a set of Fourier functions. Circuitry was also constructed so that linear systems can be synthesized by expansions in terms of these sets of functions.

A synthesis system of this type has many applications in communication studies. For example, it can be used in the representation and analysis of signals,[1,2] in the synthesis of linear systems,[3] in the synthesis of the memory portion of nonlinear systems,[4] and in the measurement of correlation functions.[5,6]

2. Method of Synthesis

The method of synthesizing these functions is described in detail by Lee.[3] In summary, if the general term of the set of Laguerre functions is written in the form

$$L_n(s) = \frac{\sqrt{2p}}{2\pi} \frac{1}{p+s} \left(\frac{p-s}{p+s}\right)^n, \tag{1}$$

it is evident that a network with the transfer function (1) can be realized by means of a lag network followed by n pure phase-shift networks in cascade. Furthermore, the $(n+1)^{\text{th}}$ term can be realized simply by the addition of another pure phase-shift network to the chain. A synthesis system for expansion in terms of the Laguerre functions is then obtained by incorporating adjustable coefficients and an algebraic summing circuit.

A set of Fourier functions that are closely related to the Laguerre functions have the general term[3]

$$F_n(s) = \frac{1}{2\pi} \left(\frac{p-s}{p+s}\right)^n. \tag{2}$$

Clearly, a synthesis system in terms of this set can be obtained from the Laguerre realization simply by bypassing the initial lag network.

Lee[3] shows that an orthonormal set of exponential functions has the general term

$$U_n(s) = \frac{\sqrt{2np}}{2\pi}\left(\frac{p-s}{p+s}\right)\left(\frac{2p-s}{2p+s}\right)\cdots\left(\frac{[n-1]p-s}{[n-1]p+s}\right)\left(\frac{1}{np+s}\right). \tag{3}$$

Inspection of this expression shows that each term is common to all previous terms except for the factor $\left(\frac{1}{np+s}\right)$. A network realization is therefore possible in the form of a phase-shift chain followed by a lag network for each term.

3. Block Diagram of Synthesizer

A block diagram of the synthesis system is shown in Fig. XIII-10. It is evident that the circuit can be modified by means of switches and capacitance to obtain the 3 sets of functions. For the exponential set, it is necessary to interchange the coefficient potentiometers and the lag networks because of the impedance levels involved. This change

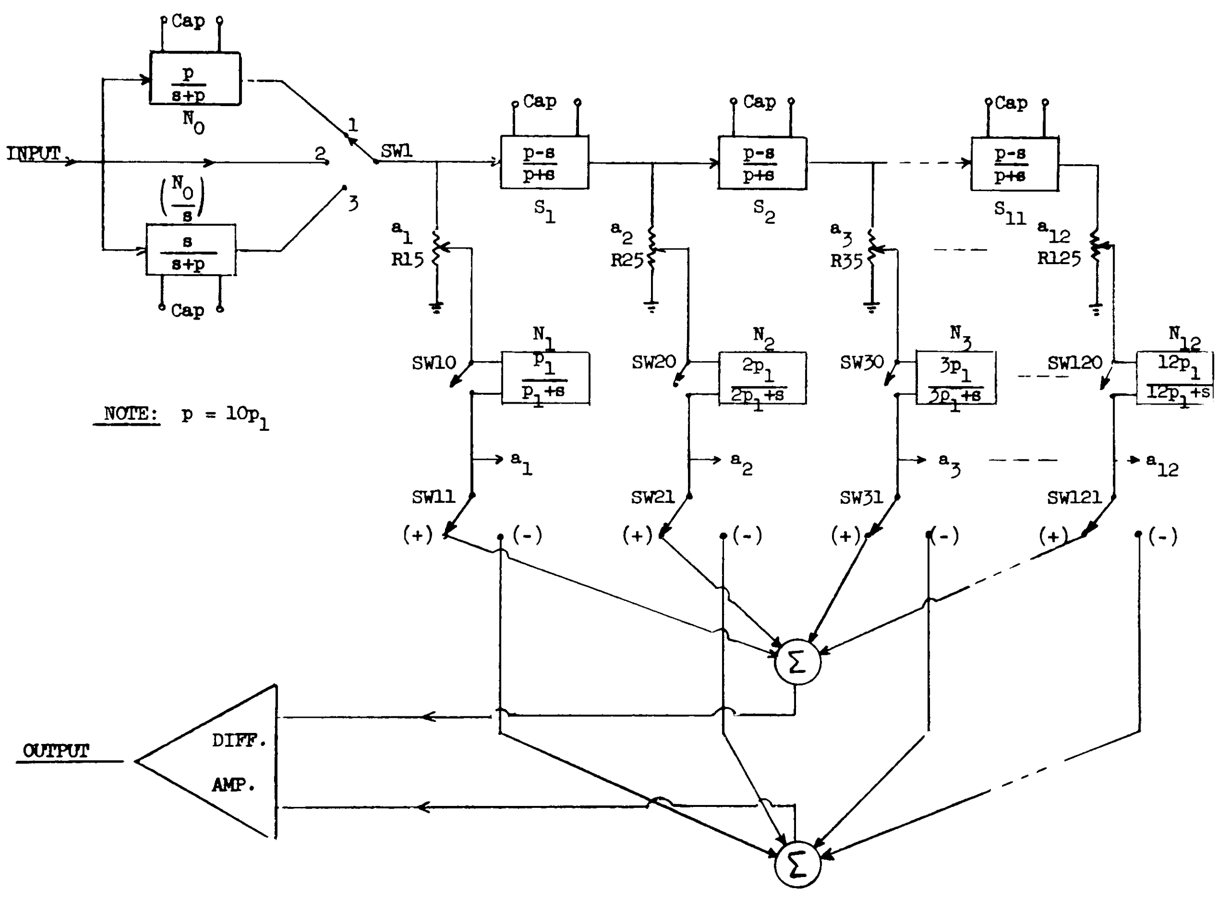

Fig. XIII-10. Linear system synthesizer block diagram.

does not affect the operation of the synthesis system in any way. The input selector switch, SW1, is set to position 1 for the Laguerre set, and to position 2 for the Fourier and exponential sets. With SW1 in position 3, the impulse responses of the Laguerre networks can be observed in response to a step input.

All of the phase-shift networks, S_1-S_{11}, have the same scale factor, p, for the Laguerre and Fourier sets. To obtain the exponential set, additional capacitance and the lag networks, N_1-N_{12}, are switched into the circuit by means of SW10, 20, ..., 120. The coefficients are adjusted by means of potentiometers R15, 25, ..., 125. The coefficient read-out (a_1, a_2, ..., a_{12}) is placed after the lag networks for alignment purposes.

Since the coefficients may be either positive or negative, two summing networks are provided. Each term may be connected to either summing circuit by switches SW11, 21, ..., 121. The outputs of the two summing circuits are then connected to a single-ended difference amplifier, by which the resultant of all the negative coefficients is conveniently inverted.

4. Description of the Circuit

The schematic diagram for the linear system synthesizer is shown in Fig. XIII-11. Vacuum tubes rather than transistors are used primarily to obtain maximum isolation between phase-shift networks with a minimum of components. The input signal to the system desirably should have an amplitude from 10-50 volts peak.

a. Input Circuitry

A cathode-follower input stage is used to prevent the source impedance from affecting the time constant of the lag network composed of R4, R5, and C1. This network is the realization of N_o in the block diagram of Fig. XIII-10. Potentiometer R5 is a fine adjustment for exactly setting the time constant of the lag network. The cathode follower also enables the dc level at the grid of V1 to be shifted to approximately −32 volts. Potentiometer R2 is adjusted so that the cathode voltages of tubes V1-V12 match the Zener diode voltages A_1-A_{12} as closely as possible.

b. Pure Phase-Shift Networks

One of the most important aspects of the circuit design was the realization of a good phase-shift network. Of the alternative methods that can be used, of which some are described by Witte[7] the active RC bridge circuit shown in Fig. XIII-12 was selected. This network, suggested by Huggins,[1] has the advantages that the input and output are single-ended, the capacitor blocks the plate voltage from the succeeding stage, feedback resulting from cathode resistance provides excellent stabilization, the gain of the stage is very nearly unity, and linear operation is achieved over a large dynamic range.

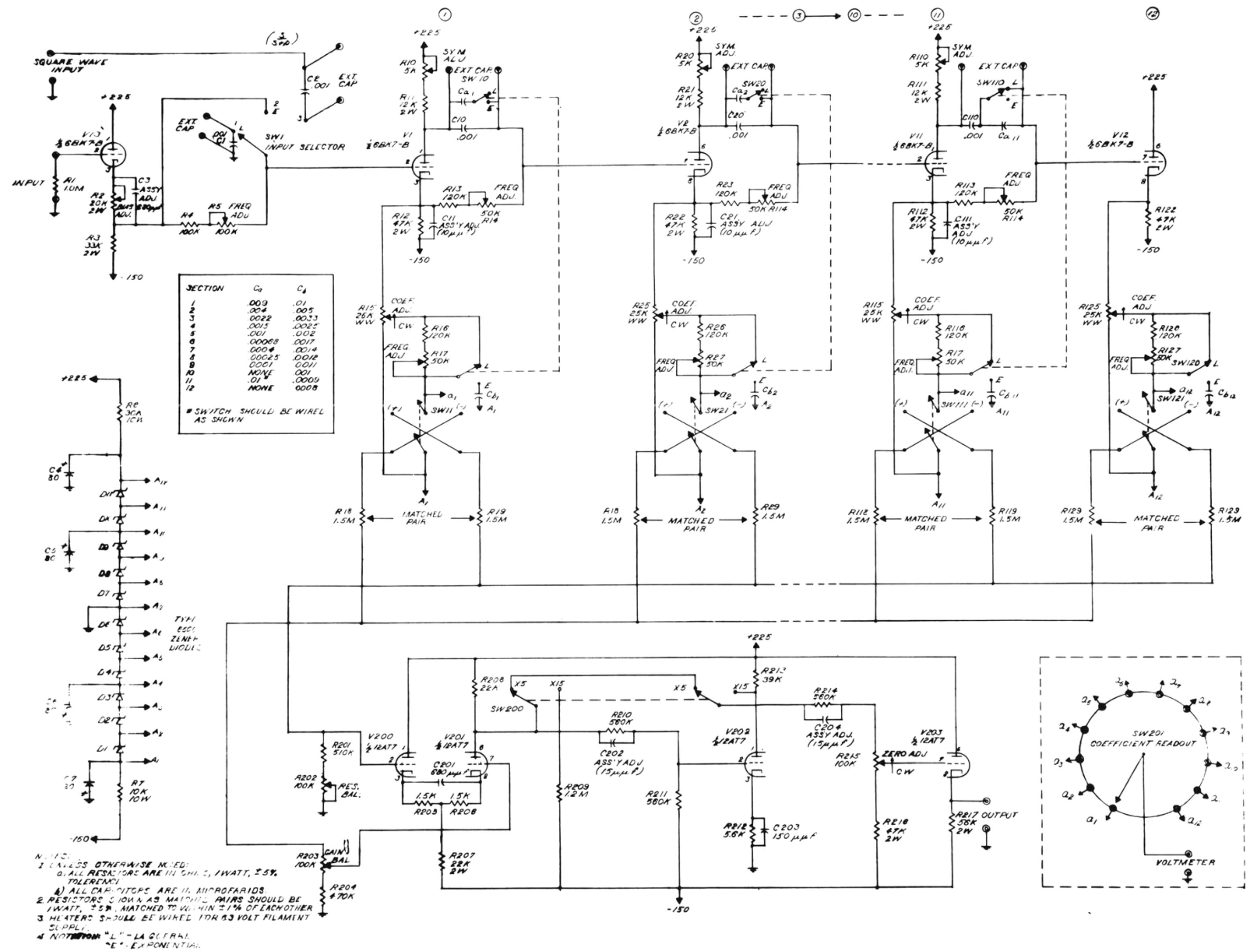

Fig. XIII-11. Schematic drawing of linear system synthesizer.

One disadvantage is that the dc level of the output exceeds that of the input by the grid-to-cathode bias voltage.

The transfer function for this circuit has been determined to be:

$$H(s) = \frac{K(s-a)}{(s-b)} = \frac{-\mu RR_L}{RR_T + r_p(R_K+R_L)} \times \frac{s - \frac{R_K}{RR_L C}}{s + \frac{R_T}{[RR_T+r_p(R_K+R_L)]C}}, \tag{4}$$

where

$$R_T = (\mu+1) R_K + r_p + R_L.$$

In order to obtain all-pass characteristics, component values must be chosen so that $a = b$. Expressing R_T, which is independent of R, in the form

$$R_T = (\mu+\delta) R_K, \tag{5}$$

where

$$\delta = 1 + \frac{r_p}{R_K} + \frac{R_L}{R_K},$$

one obtains as the criterion for a symmetrical pole-zero pattern on the real axis of the s-plane

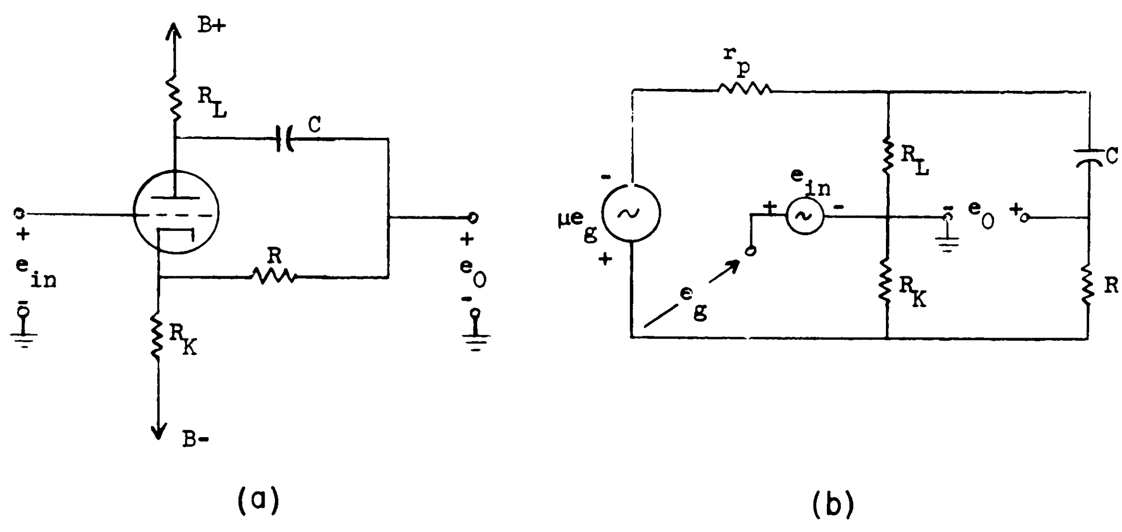

Fig. XIII-12. Active RC synthesis of pure phase-shift network. (a) One-tube realization of $H(s) = \frac{K(s-a)}{(s+b)}$. (b) Incremental circuit drawn as a bridge network.

$$R_L = R_K \times \left[\frac{\left(g_m + \frac{\delta}{r_p}\right) R + 1}{\left(g_m + \frac{\delta}{r_p}\right) R - 1}\right]. \tag{6}$$

It is interesting that the criterion (6) can also be obtained by requiring that the magnitude of the transfer function (4) at dc equal the magnitude at infinite frequency.

The circuit has been designed so that $\left(g_m + \frac{\delta}{r_p}\right) R \cong g_m R \gg 1$. Therefore, as indicated by Eq. 6, $R_L \cong R_K$, and the transconductance of the tube has very little effect on the equality of a and b. Furthermore, with reference to Eq. 4, it is seen that

$$a = b \cong \frac{1}{RC} \qquad \text{for} \begin{cases} g_m R \gg 1 \\ R_L \cong R_K . \end{cases} \tag{7}$$

Thus, as long as the conditions leading to the result (7) remain satisfied, the pole and zero locations of the transfer function (4) can be varied symmetrically about the imaginary axis of the s-plane as a function of either R or C.

The component values which were chosen for the phase-shift networks are shown in Fig. XII-11. The 5k potentiometer in the plate circuit of each stage primarily varies the location of the zero of H(s) in (4) to make a = b. A fine adjustment for setting the scale factor, p, is provided by the 50k potentiometer in the RC branch of the circuit. For a large change in scale factor, such as in converting to the exponential set, additional capacitance is used.

c. Phase-Shift Chain

It was felt that the system would be most useful if as many terms as possible of the orthogonal expansions were constructed. The decision to build 12 terms was based primarily on the estimated attenuation in gain per stage of 0.95. Assuming that this is also the gain of the cathode-follower buffer amplifier associated with the last term, the over-all attenuation of the phase-shift chain for 12 terms would be $(0.95)^{12} = 0.54$. This decrease in gain should permit the coefficient potentiometers for all terms to be adjusted over a reasonable range without requiring any intermediate stages of amplification. The fact that the plate voltage for each successive stage decreases by the same factor as the gain results in a constant dynamic range for the entire phase-shift chain.

The main problem encountered in the cascading of the phase-shift networks is the increase in the dc level at the output of each stage by the grid-to-cathode bias voltage. This makes it impractical to connect the coefficient potentiometers from the cathode of each stage to ground, as a change in setting would be accompanied by a significant change in dc level in most cases. The coefficient potentiometers, therefore, are connected to a Zener diode string that matches the dc cathode bias voltages.

With reference to Fig. XIII-11, capacitors C4 through C7 are used to prevent cross talk between terms at frequencies above 20 cps. At frequencies below 20 cps, however, some coupling between terms exists. Since the outputs of all of the phase-shift networks are very nearly in phase at low frequencies, a circuit is at present being designed to cancel this signal by means of an out-of-phase component.

d. Adjustable Coefficients

Attenuators rather than variable-gain amplifiers have been used for the adjustable coefficients for better drift stability. It should be noted that the output of each phase-shift network is taken from the cathode of the succeeding stage. This arrangement eliminates the need for buffer amplifiers to prevent loading of the phase-shift chain, and at the same time provides a low source impedance (475 ohms) for the coefficient potentiometers. A cathode follower is necessary only for the final phase-shift network.

For the Laguerre and Fourier sets, the setting of the coefficients has no effect on the summing circuit, which has an input impedance of 1.5 megohms for either polarity. Similarly, the summing circuit does not cause any disturbance in the phase-shift chain in varying the coefficient settings.

The system has been provided with a rotary switch that enables the settings of the coefficient potentiometers to be either adjusted or measured in cyclic order. As previously mentioned, the coefficient read-out has been placed after the lag networks of the exponential set for alignment purposes.

e. Lag Networks

The lag networks for the exponential set are formed by switching the capacitors, C_b, into the circuit and, at the same time, switching the resistance in series with the arm of the coefficient potentiometers. A fine adjustment for the scale factor of the lag networks is provided by the 50k potentiometers. The values of C_a and C_b listed in the table in Fig. XIII-11 are calculated to give a fundamental scale factor, $p_1 = 2\pi \times 100$ rad/sec.

Impedance levels between the coefficient potentiometers, the lag networks, and the summing circuit differ only by factors of 10. Thus, in using the exponential set, the effect of one portion of the synthesis system on another should be taken into account for best accuracy. In the future, it would be desirable to incorporate some changes in the circuit to improve this situation.

f. Summing Circuit

Passive summation has been used to minimize the number of active circuit elements and their associated drift. Two summing circuits are employed in which all positive coefficients are combined in one group and all negative coefficients in the other, as shown in Fig. XIII-10. The two summing circuits are identical, so that each term can be connected to either circuit, as desired, without affecting the other. As shown in Fig. XIII-11, this is accomplished with a double-pole, double-throw switch and a pair of matched resistors for each term. Potentiometer R202 is used to adjust for any differences that might exist between the two summing circuits.

In connection with the double-pole, double-throw polarity switches, a suggestion for future systems is to use three-position toggle switches (+, off, −). It would then be possible to disconnect terms in the orthogonal expansion without destroying coefficient settings. This would facilitate an investigation of the contribution of a given term in the expansion to the over-all impulse response of the system.

g. Difference Amplifier

The outputs of the two summing circuits are connected to a cathode-coupled difference amplifier to complete the synthesis system. In this way, the sum of all terms whose coefficients are negative are conveniently subtracted from the sum of the remaining terms whose coefficients are positive. The use of a difference amplifier as an input stage tends to minimize drift resulting from plate-supply and filament-voltage variations, and also makes it possible to convert a balanced input to a single-ended output. Potentiometer R203 is used to equalize the gains with respect to both amplifier inputs.

The difference amplifier is followed by a stage of additional amplification, if needed, and a cathode-follower output stage. Coupling between stages is by means of resistive divider networks to obtain proper biasing. Capacitors C202, C203, and C204 are selected to compensate for the attenuation in gain at high frequencies.

5. Results and Conclusions

The synthesis system was constructed in a chassis that is suitable for rack-mounting. The circuit was then checked out stage by stage and aligned according to a procedure previously described.[7] The over-all performance indicates that the objective has been achieved of designing and building a system for representing system functions whose frequency spectrums are primarily confined to the audio range.

a. Bandwidth Considerations

In order to represent systems functions with the Laguerre functions at frequencies relatively high as compared with the scale factor, higher-order terms are required. To verify this statement, assume that we wish to represent a system function, $H(\omega)$, whose frequency spectrum extends to roughly $\omega = kp$ rad/sec, by means of a set of Laguerre networks. The Fourier transform of the impulse response of the n^{th}-order network is

$$L_n(\omega) = \frac{(p-j\omega)^n}{(p+j\omega)^{n+1}} = \frac{1}{\sqrt{p^2+\omega^2}} \, e^{-j2n\,\phi(\omega)} \tag{8}$$

where

$$\phi(\omega) = \tan^{-1}\frac{\omega}{p} .$$

At the frequency, $\omega = kp$, where $k \gg 1$,

$$\phi(\omega)\Big|_{\omega = kp} = \tan^{-1} k\Big|_{k \gg 1} \cong \left(\frac{\pi}{2}-\frac{1}{k}\right) \text{ radians} \tag{9}$$

and

$$L_n(\omega)\Big|_{\omega = kp} \cong \frac{(-1)^n}{p\sqrt{1+k^2}} \; e^{j2n/k} \tag{10}$$

From Eq. 10 we conclude that if k is large, n must also be large in order to have sufficient phase response at $\omega = kp$ for satisfactorily characterizing $H(\omega)$ at that frequency. In other words, for a given scale factor, the frequency range that can be accomodated by the Laguerre networks is determined by the number of terms.

It is also evident from this result that one disadvantage of the cascade method of synthesis is that the over-all bandwidth decreases as the number of terms increases. Thus, for a given bandwidth per stage, a definite limit on the number of terms is imposed if the effects of high-frequency magnitude and phase distortion are to be avoided. In the synthesis system that was constructed, the bandwidth for 11 phase-shift networks in cascade is approximately 15 kc. For a scale factor of $p = 2\pi \times 1000$ rad/sec, the phase response at 15 kc at the output of the eleventh all-pass network is within $\frac{\pi}{2}$ radians of its asymptotic high-frequency value of -11π radians. Thus, the system has sufficient bandwidth to represent functions over the frequency range in which most of the phase shift takes place, that is, from approximately 100 cps to 10 kc. Several additional terms, however, might decrease the over-all bandwidth so that high-frequency magnitude and phase distortion would occur. For the exponential set, the scale factor of the phase-shift networks increases with successive terms. This tends to accentuate the effect of the decreasing over-all bandwidth even more than with the Laguerre set.

b. Response of the Laguerre Networks

As a demonstration of the performance of the system, photographs of the impulse responses of the network realizations of the Laguerre functions are shown in Fig. XIII-13. These functions were obtained in response to a step input, so that the problem of generating a "satisfactory" impulse in the laboratory was avoided. Also, the possibility of saturating the cathode-follower input stage (V13) with a large voltage spike is avoided.

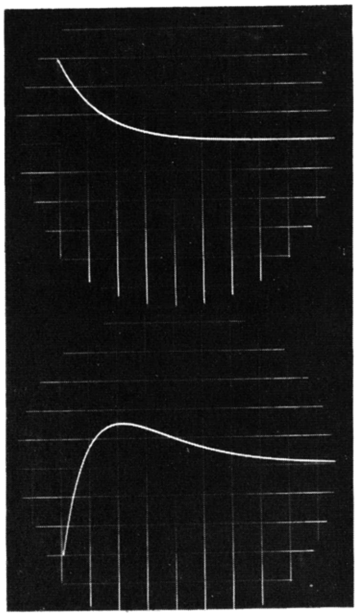

n = 0, 1
p = 2π × 1000 rad/sec
t = 0.1 msec/cm

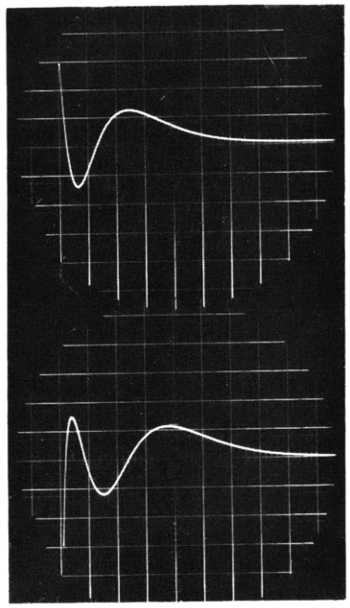

n = 2, 3
p = 2π × 1000 rad/sec
t = 0.2 msec/cm

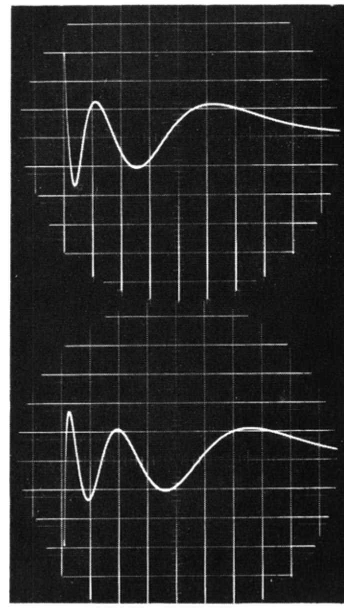

n = 4, 5
p = 2π × 1000 rad/sec
t = 0.2 msec/cm

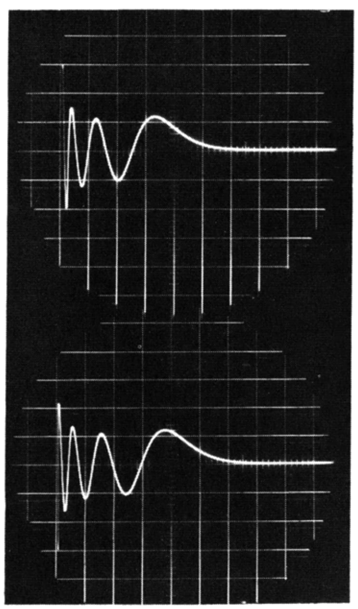

n = 6, 7
p = 2π × 1000 rad/sec
t = 0.5 msec/cm

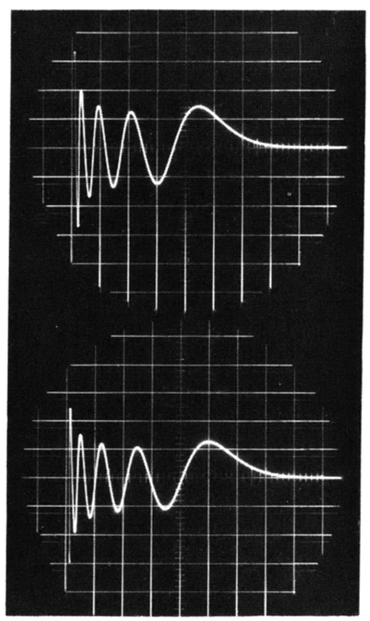

n = 8, 9
p = 2π × 1000 rad/sec
t = 0.5 msec/cm

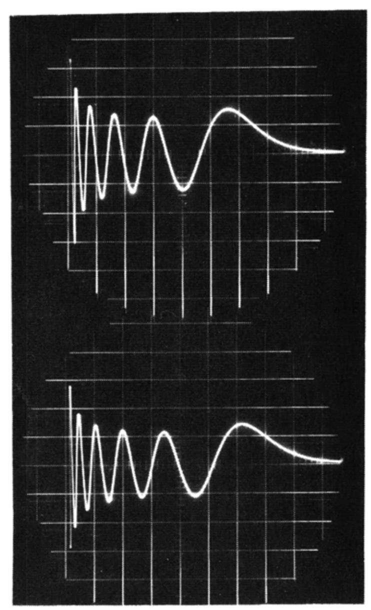

n = 10, 11
p = 2π × 1000 rad/sec
t = 0.5 msec/cm

Fig. XIII-13. The Laguerre functions $\{l_n(t)\}$.

Inspection of the waveforms in Fig. XIII-13 shows that the initial values alternate as they should for successive terms according to $(-1)^n$, in which n is the order of the term in the set, $\{\ell_n(t)\}$. Close inspection of the photographs also verifies that the number of zero crossings for each term is equal to the designating subscript of the function. It is interesting to note that the peaks of the sixth- and higher-order terms do not decrease monotonically, as might be expected from the nature of the first few terms. It can also be seen that higher frequency components are evidenced as the order of the terms increases. Each set of three functions in Fig. XIII-13 has the same time scale. Comparison of the first 6 terms with actual plots of the functions shows that they are in close agreement. A tabulation through the eighth term also indicates close agreement.

R. W. Witte

References

1. W. H. Huggins, Representation and Analysis of Signals: Part I, The Use of Orthogonal Exponentials, Report AFCRC TR-57-357, Johns Hopkins University, Baltimore, Md., September 1957.

2. D. C. Lai, Representation and Analysis of Signals: Part II, An Orthonormal Filter for Exponential Waveforms, Report AFCRC TR-58-191, Johns Hopkins University, Baltimore, Md., June 1958.

3. Y. W. Lee, Statistical Theory of Communication (John Wiley and Sons, Inc., New York, 1960).

4. N. Wiener, Nonlinear Problems in Random Theory (The Technology Press of Massachusetts Institute of Technology, Cambridge, Mass., and John Wiley and Sons, Inc., New York, 1958).

5. D. G. Lampard, A New Method of Determining Correlation Functions of Stationary Time Series, Monograph No. 104, August 16, 1954, Proc. Inst. Elec. Engrs. (London) 102C, 35-51 (1954).

6. M. Schetzen, Some Problems in Nonlinear Theory, Sc.D. Thesis, Department of Electrical Engineering, M.I.T., May 20, 1961; Technical Report 390, Research Laboratory of Electronics, M.I.T., July 6, 1962.

7. R. W. Witte, Synthesis of Several Sets of Orthogonal Functions, S.M. Thesis, Department of Electrical Engineering, M.I.T., May 21, 1962.